Study on the regulatory mechanism for Uncoupling protein 1 (Ucp1) expression in beige adipocytes

Ana Yuliana

2019

Contents

Abbreviations

Adrb3	adrenoceptor beta 3
ADP	adenosine diphosphate
ATP	adenosine triphosphate
β-AR	beta-adrenergic receptor
BAT	brown adipose tissue
Bip	binding immunoglobulin protein
cAMP	cyclic adenosine monophosphate
ChIP	chromatin immunoprecipitation
Chop	CCAAT-enhancer-binding protein homologous protein
COXIV	cytochrome c oxidase subunit IV
CRE	cAMP response element
DG	diacylglycerol
ER	endoplasmic reticulum
ERAD	ER-associated degradation
ERK	extracellular signal-regulated kinase
ETC	electron transport chain
FFA	free fatty acid
H3ac	histone H3 acetylation
H3K27ac	histone H3 lysine 27 acetylation
H&E	hematoxylin and eosin
HDAC	histone deacetylase
HDI	HDAC inhibitor
IHC	immunohistochemistry
IRE1α	inositol-requiring enzyme 1 alpha
iso	isoproterenol
IWAT	inguinal white adipose tissue
JNK	c-Jun N-terminal kinase
lac	lactacystin
MAPK	mitogen-activated protein kinase
MG	monoacylglycerol
PBA	4-phenylbutyrate
Pgc1α	peroxisome proliferator-activated receptor gamma coactivator 1 alpha

p-HSL	phospho-hormone-sensitive lipase
PKA	protein kinase A
PPAR	peroxisome proliferator-activated receptor
PPRE	PPAR response element
rosi	rosiglitazone
S112	serine 112
siRNA	small interfering RNA
SNS	sympathetic nervous system
T3	triiodo-L-thyronine
TG	triacylglycerol
tun	tunicamycin
UCP1	uncoupling protein 1
UPR	unfolded protein response
WAT	white adipose tissue
Xbp1	X-box binding protein
Xbp1s	spliced XBP1

General introduction

The economic and social growth, which marked through the increasing urbanization and rising income, have brought a new sedentary lifestyle worldwide. People nowadays have less time to exercise or prepare food. Consequently, the demand for a calorie-dense food, which is labeled as “more convenient food” is rising and becoming more popular. The new eating habits and lifestyle are believed to be the main cause of a drastic increase in the overweight-obesity cases worldwide. World Health Organization of United Nation’s recent estimation states that 1.9 billion adults are overweight of whom over 650 million are obese. Obesity has been represented as one of most important public health problems due to its associated risk of the progression of other diseases such as insulin resistance, type-2 diabetes, fatty liver, cardiovascular diseases, and cancer. All these factors hence urge us to find a new therapeutic strategy for obesity management.

Obesity is broadly defined as an abnormal or excessive accumulation of fat in adipose tissue. Adipose tissue is an important organ that responds to the changes in nutrient supply such as overfeeding or starvation. For decades, adipose tissue has been known not only as energy storage, but also as an active endocrine program, which secretes cytokines and hormones involved in the regulating metabolic processes [1,2]. Generally, adipose tissue has been characterized into white adipose tissue (WAT) and brown adipose tissue (BAT) with different morphology, distribution, gene expression, and function [3,4]. The development of obesity, in fact, not only depends on the balance between energy consumption and expenditure, but also the balance between WAT and BAT [5].

WAT has been characterized with low oxidative capacity and mainly functions to maintain energy homeostasis by storing excess lipid as triglycerides in time of overfeeding, which can be released as non-esterified fatty acid in the starving period to fulfill the demand of energy [1,3]. All white adipocytes contain a single large lipid drop that takes up into 90% of the cells volume

with few mitochondria. Due to its primary function as the main energy reservoir, WAT have considerable capacity to expand in response of the surplus of energy. In obese condition, however, the excessive accumulation of fat could exceed the limit of WAT expansion and functionality, disturbing energy homeostasis and result in WAT dysfunctionality and ectopic deposition of toxic lipid in other metabolic organs such as the liver, heart, and muscles [1,6]. Hence, these factors start the onset and the progression of obesity associated-metabolic diseases.

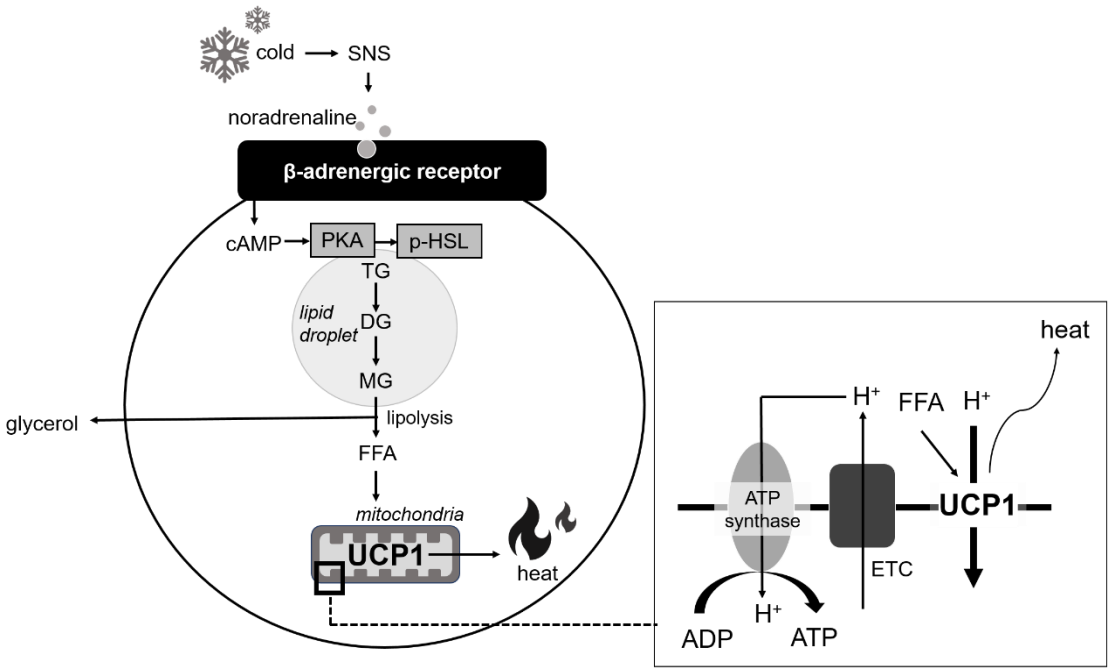

Figure 1. A key metabolic pathway of non-shivering thermogenesis.
SNS: sympathetic nervous system; cAMP: cyclic adenosine monophosphate; PKA: protein kinase A; p-HSL: phospho-hormone-sensitive lipase; TG: triacylglycerol; DG: diacylglycerol; MG: monoacylglycerol; FFA: free fatty acid; UCP1: uncoupling protein 1; ADP: adenosine diphosphate; ATP: adenosine triphosphate; ETC: electron transport chain.

In the opposite of WAT, BAT is packed with high amounts of mitochondria and oxidative capacity, thus specialized in energy expenditure rather than energy storage. BAT contains multiple and small lipid droplets. Besides nutrient supply, adipose tissue also responds to the ambient temperature to maintain the core body temperature when exposed to temperatures below thermoneutrality. Indeed, BAT is known as a key site for heat production in a process called non-

shivering thermogenesis [3,7]. In cold conditions, the sympathetic nervous system (SNS) releases noradrenaline, a catecholamine that can bind and induce β-adrenergic receptor (β-AR) stimulation, thus subsequently activating BAT function to burn fatty acid from lipid droplets (lipolysis) and convert the energy in the form of heat [3,6] (Figure 1). Further, this thermogenesis mechanism was mediated crucially by uncoupling protein 1 (UCP1).

UCP1 is a mitochondrial membrane transporter protein located in the inner mitochondria. Hence, it is highly expressed in the mitochondria-packed BAT, but not in WAT. The thermogenic capacity of BAT is regulated through β-AR activation-cyclic adenosine monophosphate (cAMP) dependent pathways which lead to the production of fatty acids [8] (Figure 1). These fatty acid is a critical switch to stimulate UCP1 expression [8,9]. When activated, UCP1 will uncouple oxidative phosphorylation in cellular respiration, resulting in energy dissipation in the form of heat, instead ATP [2] . Because of this crucial role, UCP1 often used as BAT activation marker and has been targeted for obesity management. Human BAT is highly present in infants (neonatal period) to primarily maintain their body temperature and warm the blood flowing through of key organs, therefore preventing hypothermia [6]. In adults, however, BAT functions are negligible and its depots are re-discovered with the mixtures of white and beige adipocytes [5,10]. Indeed, recent studies showed the appearance of inducible brown-like white adipocytes (known as beige adipocytes) especially in certain depots of WAT when exposed to β-AR stimulation. This process is referred to as browning of WAT. Recent findings found that the third type of adipocytes, beige adipocytes are not derived from the same lineage as BAT [5]. Further, beige adipocytes are characterized by low expression of UCP1 in the basal level (WAT-like) but can have high UCP1 expression when stimulated (BAT-like) [7,11–13]. Thus, browning of WAT is marked by the upregulation of UCP1 expression.

Given to these newly found phenomena, preventing the impairment of or enhancing *Ucp1* expression in beige adipocytes will increase the thermogenesis capacity in adipose tissue, and subsequently affect the whole-body energy metabolism, thus possibly being beneficial for obesity

prevention. Hence, a deeper and more comprehensive understanding about the mechanism of *Ucp1* expression regulation in beige adipocytes might help for better obesity management. In this report, the potential mechanisms that could lead to the improvement of *Ucp1* expression in beige adipocytes will be investigated (Figure 2).

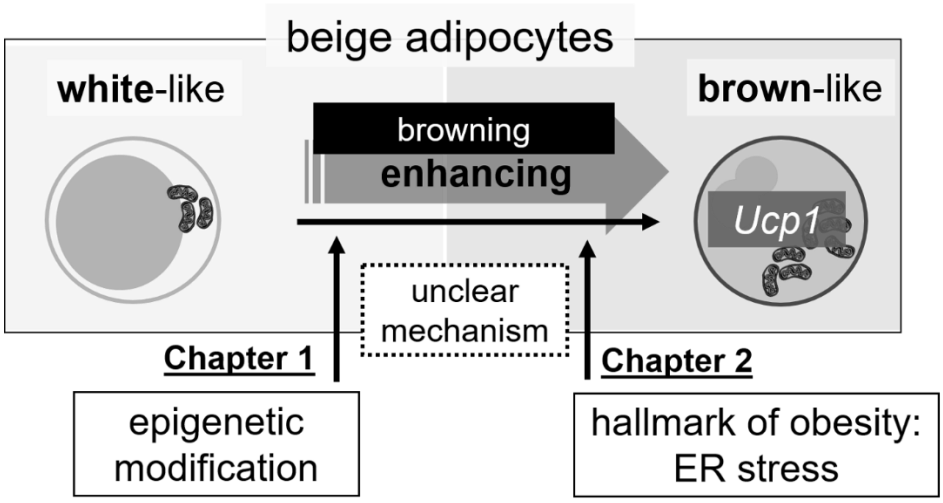

Figure 2. The objective scheme of the present study.
The involvement of epigenetic modification and endoplasmic reticulum (ER) stress in regulating adipocytes browning marker–*Ucp1* expression in beige adipocytes will be investigated in Chapter 1 and Chapter 2, respectively.

As the classic BAT or beige activator, cold exposure, is not convenient to do in human therapeutic strategy, several pharmacological drugs have been developed to stimulate browning in ambient temperature. Among those drugs, β–AR agonist have been widely used for induction of browning, although there are concerns about the side effects [14]. Thus, finding a new molecular target to induce or enhance WAT browning is still needed. Accordingly, there is an accumulated evidence that epigenetic modifications could also stimulate browning of WAT, although the mechanism is still unclear. Epigenetics is a new approach of study that investigates gene regulation through chromatin remodeling and has been targeted to treat diseases such as obesity and cancer [15–17]. This study thus aims to examine the involvement of epigenetic regulation in regulating *Ucp1* expression in beige adipocytes. Indeed, we found a novel potential

target involving epigenetic modifications to enhance *Ucp1* expression in beige adipocytes, which will be presented thoroughly in Chapter 1.

In addition to epigenetic regulation, it has been known that physiological condition such as obesity could also influence *Ucp1* expression. However, obesity is characterized by a variety of metabolic symptoms such as endoplasmic reticulum (ER) stress and many more [18,19], and thus a specific factor that could regulate *Ucp1* expression is still unclear. ER stress is marked by the accumulation of unfolded protein that subsequently triggers unfolded protein response (UPR) [20]. Since UPR can trigger various signaling pathways, there is a possibility that the thermoregulation in beige adipocytes is also affected. In this study, we found a novel regulation of ER stress in regulating *Ucp1* expression in beige adipocytes. An additional necessary target to improve *Ucp1* expression through ER stress regulation will be carefully described in Chapter 2.

Chapter 1

β-adrenergic receptor stimulation suppressed histone deacetylase 3 to induce uncoupling protein 1 expression[1]

Introduction

Recently, browning of white adipose tissue (WAT) has garnered attention as a potent target for obesity. The term "browning" originated from the distinct characteristics of WAT and brown adipose tissue (BAT). WAT shows low oxidative capacity to support the storage of excess energy as triglyceride, while by contrast, BAT shows high oxidative capacity due to high mitochondrial content. Beige adipocytes develop within WAT in response to β-adrenergic receptor (β-AR) stimulation, such as cold conditions to activate a thermogenesis program to produce heat by increasing energy expenditure [4,12]. This phenomenon would be beneficial for obesity, as WAT has a relatively large mass, and therefore any change in cell physiology in this tissue may affect whole body metabolism. Once activated, beige adipocytes exhibit similar functional thermogenic characteristics as BAT, and thus browning is marked by upregulation of browning-fat specific genes, such as uncoupling protein 1 (*Ucp1*) [4,7,13]. The increased *Ucp1* expression in beige adipose tissue is especially evident in the inguinal region where basal level of *Ucp1* is very low [21,22]. Many efforts have been made to pharmacologically stimulate the thermogenesis program through β-AR agonists, especially β3-AR. However, β3-AR agonists lack efficacy in human translational studies [10,23,24]. Hence, finding a new molecular target to induce browning is needed.

---

[1]The content described in this chapter was originally published in International Journal of Molecular Sciences (IJMS). Yuliana A, Jheng HF, Kawarasaki S, Nomura W, Takahashi H, Ara T, Kawada T, and Goto T. β-adrenergic Receptor Stimulation Revealed a Novel Regulatory Pathway via Suppressing Histone Deacetylase 3 to Induce Uncoupling Protein 1 Expression in Mice Beige Adipocyte. *Int. J. Mol. Sci.* (2018), 19(8):2436, 1-15. doi:10.3390/ijms19082436

Epigenetic modification has emerged as a new approach to treat diseases including cancer and obesity, by the remodeling of chromatin structure through mechanisms such as acetylation of lysine on histones. Histone is a protein that acts as a spool that packages DNA into nucleosomes and chromatin. Acetylated histone provides binding sites for transcription factors by neutralizing histone positive charges and loosening the interaction between histone and DNA, thus promoting gene expression [25]. Acetylation of histone H3 lysine 27 (H3K27ac) is known as a potent activation mark for browning-related genes, such as *Ucp1* [26–29]. H3K27ac distinguish active enhancers by allowing higher DNA access (open chromatin), which favors transcriptional activation [29–31]. Conversely, histone deacetylation condenses chromatin structure, suppressing gene expression [32,33]. Deacetylation of histone is mainly mediated by enzymes called histone deacetylase (HDAC) [33]. So far, there are 18 mammalian classical Zn^{2+}-dependent HDAC that have been characterized and divided into four classes (class I–IV) based on similarity in structure to yeast HDAC [33]. Although structurally similar, the function of each HDAC homologue might differ depending on the complex HDAC formed.

Interestingly, there is accumulating evidence that HDAC inhibitor (HDI) can stimulate browning of adipose tissue in BAT and WAT [17,26,27,34–38] which suggest the inhibition of HDAC might be closely related to browning. However, the detailed mechanism is still unclear and how β-AR stimulation might regulate HDAC activity is unknown. Indeed, in this study we show for the first time that β-AR stimulation also triggers similar HDAC inhibitory activity that benefited *Ucp1* expression in beige adipocytes.

Materials and methods

Materials

All chemicals were obtained from Nacalai Tesque (Nacalai Tesque, Kyoto, Japan), Wako (Wako Pure Chemicals, Osaka, Japan), Corning (Corning, Corning, NY, USA), Qiagen (Qiagen, Hilden, Germany), Invitrogen (Invitrogen, Carlsbad, CA, USA), and Sigma-Aldrich (Sigma-

Aldrich, St. Louis, MO, USA). TM251 was purchased from Active Motif (Active Motif, Tokyo, Japan). PCI34051 and RGFP966 were acquired from Cayman (Cayman Chemical, Ann Arbor, MI, USA).

Animal experiment

Mice were kept in a temperature-controlled room at 23 ℃ ± 1 ℃ with a 12 h light/dark cycle and free access to food (standard diet) and water. To stimulate β-AR activation, 14-week-old male C57BL/6N mice (SLC, Shizuoka, Japan) were exposed to cold (10 ℃). Mice were sacrificed and inguinal white adipose tissue (IWAT) was harvested for mRNA and protein analysis. The mice were handled in accordance with procedures approved by the Animal Research committee of Kyoto University (Permission number: 29–62; 20 April 2012).

Cell culture

Primary pre-adipocyte of IWAT was immortalized by transfecting pBabe-puro largeTcDNA retrovirus containing SV40 largeT antigen. Successfully transfected clone was screened based on puromycin resistance. Immortalized primary inguinal white adipose tissue cell (IWAT cells) was maintained in a humidified 5% CO_2 atmosphere at 37 ℃ using basic medium (DMEM) supplemented with 10% fetal bovine serum and 1% penicillin/streptomycin. Maintenance medium consisted of basic medium supplemented with 0.25 μg/mL puromycin. Two days after confluence, cells were differentiated by stimulation with 0.5 mM 1-methyl-3-isobutylxanthine, 0.25 μM dexamethasone, 10 μg/mL insulin, 1 nM triiodo-L-thyronine (T3), 0.5 μM rosiglitazone (Rosi), and 125 μM indomethacin for 48 h. The media was then replaced by growth medium (basic medium containing 5 μg/mL insulin, 1 nM T3, and 0.5 μM Rosi) for another 48 h. After that, the media was changed every 2 days with basic medium supplemented

with 5 μg/mL insulin and 1 nM T3. Generally, the differentiation process took 6–7 days. β-AR stimulation was induced by isoproterenol addition in serum free medium.

RNA preparation and quantification of gene expression

RNA was prepared and quantified as previously described [39,40]. Total RNA was extracted from cultured cells in 12-well plates or tissue according to the phenol-chloroform extraction method. RNA expression was quantified by real-time PCR using a LightCycler System (Roche Diagnostics, Mannheim, Germany) with SYBR Green fluorescence signal detection. All mRNA signals were normalized to a 36b4 internal control. The primer sequences are listed in Table 1.

Table 1. Primers used for RNA quantification

Gene	Forward	Reverse
Ucp1	5'-CAAAGTCCGCCTTCAGATCC-3'	5'-AGCCGGCTGAGATCTTGTTT-3'
Adrb3	5'-GCACCTTAGGTCTCATTATGG-3'	5'-GCGAAAGTCCGGGCTGCGGCAGTA-3'
Pgc1α	5'-CCCTGCCATTGTTAAGACC-3'	5'-TGCTGCTGTTCCTGTTTTC-3'
Pparα	5'-TCGCGTACGGCAATGGCTTTT-3'	5'-CTTTCATCCCCAAGCGTAGGAGG-3'
Pparγ	5'-GGAGATCTCCAGTGATATCGACCA-3'	5'-ACGGCTTCTACGGATCGAAAACT-3'
Hdac1	5'-CCCATGAAGCCTCACCGAAT-3'	5'-CAAACACCGGACAGTCCTCA-3'
Hdac2	5'-CTGTCTCGCTGGTGTTTTGC-3'	5'-GTCATTTCTTCAGCAGTGGCT-3'
Hdac3	5'-ATGTGCCGCTTCCATTCTGA-3'	5'-TGGCATGATGTAGACCACCG-3'
Hdac6	5'-CAGCAGGATTTGCCCACCTA-3'	5'-TCTCCAGGACCTCCCAGAAG-3'
Hdac7	5'-TGGGGGATCCTGAGTACCTG-3'	5'-GTCCACCCTCTAAGGCCAAC-3'
Hdac8	5'-ACTTGACCGGGGTCATCCTA-3'	5'-AACCGCTTGCATCAACACAC-3'
Hdac9	5'-CCCACCACACATCACTGGAT-3'	5'-TCCATCCTTCCGCCTGAGTA-3'
36b4	5'-TCCTTCTTCCAGGCTTTGGG-3'	5'-GACACCCTCCAGAAAGCGAG-3'

Immunoblotting

Western blotting was performed as previously described [41]. Briefly, cells or tissue were lysed, and protein was collected after centrifugation. Protein concentration was measured using the DC protein assay (Bio-Rad, Hercules, CA, USA). Denatured protein was then separated and

transferred to a polyvinylidene difluoride transfer membrane. The membrane was then blocked, washed, and incubated with the corresponding primary antibody, followed by the appropriate secondary antibody. Anti-histone H3 (acetyl K27) (Abcam, Cambridge, UK), anti-acetyl-histone H3 (Millipore, Burlington, MA, USA), anti-histone H3 (Novus biological, Littleton, CO, USA), anti-HDAC3 (Sigma-Aldrich, St. Louis, MO, USA), and anti-β-actin (Cell Signaling Technology, Danvers, MA, USA) were used as primary antibodies. The secondary antibody staining was visualized using a chemiluminescent horseradish peroxidase substrate (Millipore, Burlington, MA, USA).

HDAC activity assay

HDAC activity was measured using an HDAC Cell-Based Activity Assay Kit (Cayman Chemical, Ann Arbor, MI, USA) as described in the manufacturer's instructions. Briefly, 1 x 10^4 differentiated IWAT cells were plated in a 96-well black plate, clear bottom (Greiner Bio-One, Kremsmünster, Austria) as recommended by the protocol, and let to set for 6 h overnight before stimulation, and then analysed for HDAC activity.

Chromatin immunoprecipitation (ChIP) assay

The ChIP assay was performed according to company protocol (Millipore, Burlington, MA, USA) with some modification. Cells were first fixed in 1% formaldehyde and then quenched by 125 mM glycine. Cells were collected and re-suspended in 1% SDS lysis buffer, and then sonicated to shear DNA into 100–1000 bp fragments. The supernatant was collected and subjected to overnight immunoprecipitation with 4 µg H3K27ac antibody (Abcam, Cambridge, UK), 25 µg HDAC3 antibody (Abcam, Cambridge, UK), or rabbit IgG isotype control (Novus Biological, Littleton, CO, USA) as a mock control, together with Magna ChIP™ Protein A+G Magnetic Beads (Millipore, Burlington, MA, USA) at 4 °C in a rotatory shaker, followed by reverse cross link and protease K digestion. Eluted DNA was then purified using a MinElute PCR Purification

Kit (Qiagen, Hilden, Germany) and analysed by real-time PCR. Primer sequences are listed in Table 2.

Table 2. Primers used in chromatin immunoprecipitation (ChIP) assay

Gene	Forward	Reverse
Ucp1 enhancer	5'-CTCCTCTACAGCGTCACAGAGG-3'	5-AGTCTGAGGAAAGGGTTGA-3'
Ucp1 proximal	5'-CCCACTAGCAGCTCTTTGGA-3'	5-CTGTGGAGCAGCTCAAAGGT-3'

Small interfering RNA (siRNA) transfection

The transfection of siRNA was performed in mature IWAT cells. After differentiation, cells were re-plated for 80% confluence in a 24-well plate. *Hdac3* and *Hdac8* siRNA (Table 3) transfection was performed according to the manufacturer's instructions (Invitrogen, Carlsbad, CA, USA) using Lipofectamine 2000 transfection reagent (Invitrogen, Carlsbad, CA, USA). Cells were collected 24 h after transfection.

Table 3. Small interfering RNA (siRNA)

Gene	Sequence
Hdac3	CAGCAUGACAUGUGCCGCUUCCAUU
Hdac8	GACGGAAAUUUGACCGUAUUCUCUA

Statistical analysis

All data were analyzed using Student's t-test or one-way ANOVA followed by Tukey-Kramer test, when variances were heterogeneous. All data are presented as means ± SEM. Differences were considered significant at $p < 0.05$.

Results

β-AR stimulation-induced acetylation of histone H3 lysine 27 favouring open chromatin structure in the *Ucp1* promoter region

β-AR were first stimulated by exposing mice to cold (10 °C) for 8 or 24 h. IWAT were then harvested. Browning in IWAT was successfully stimulated, indicated by the upregulation of

Ucp1 expression (Figure 3A). H3K27ac, a signature of histone activation, was also induced after 24 h cold exposure (Figure 3B). Furthermore, total histone H3 acetylation (H3ac), which includes several lysine sites, was also increased, suggesting a major transcriptional activation of genes during cold exposure. Similar results from the initial stage of cold exposure (0–24 h) in IWAT were also obtained in immortalized primary inguinal white adipose tissue cells (IWAT cells) treated with the β-AR agonist isoproterenol. The treatment showed an increment of *Ucp1* in time-dependent manner until 4 h (Figure 4A). On the other side, H3K27ac was also significantly increased when *Ucp1* was maximally expressed after 4 h isoproterenol addition (Figure 4B).

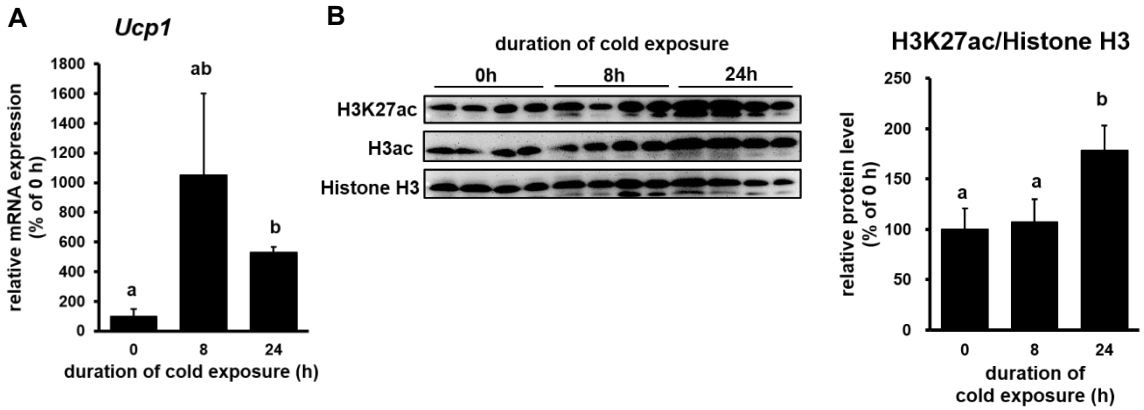

Figure 3. Histone acetylation state under cold stimulation in inguinal white adipose tissue (IWAT). (**A**) Uncoupling protein 1 (*Ucp1*) expression and (**B**) histone H3 lysine 27 acetylation (H3K27ac) level from the mice exposed to cold (10 °C) at different time points. Protein band were quantified by ImageJ. Data are presented as mean ± S.E.M. (error bars). n = 3–6 in each group. Different letters indicate significant difference ($p < 0.05$) according to one-way ANOVA followed by the Tukey-Kramer multiple comparison test. Same letters indicate non-significant difference.

To further confirm the association between the increased histone acetylation in H3K27 and *Ucp1* upregulation during β-AR stimulation, ChIP assay was performed to investigate if H3K27ac also increases within the *Ucp1* promoter region in IWAT cells. Two notable sites at the *Ucp1* promoter region (the enhancer and proximal regions) were selected to investigate histone acetylation in H3K27 and thus predict *Ucp1* chromatin state. The results showed that H3K27ac was considerably increased both in the *Ucp1* enhancer (Figure 4C) and proximal (Figure 4D)

regions. In addition, peroxisome proliferator-activated receptor (PPAR) gamma coactivator 1 alpha (*Pgc1a*) mRNA upregulation upon β-AR stimulation (Figure 4E) was also accompanied by an increase of H3K27ac in the *Pgc1a* of the cAMP response element (CRE) region, although the difference was not significant (Figure 4F). This result may indicate that H3K27ac regulates not only *Ucp1* but also other browning genes. Nevertheless, these results concluded an open chromatin structure for *Ucp1* transcriptional activation as marked by a significant increase of H3K27ac during β-AR stimulation in beige adipocytes.

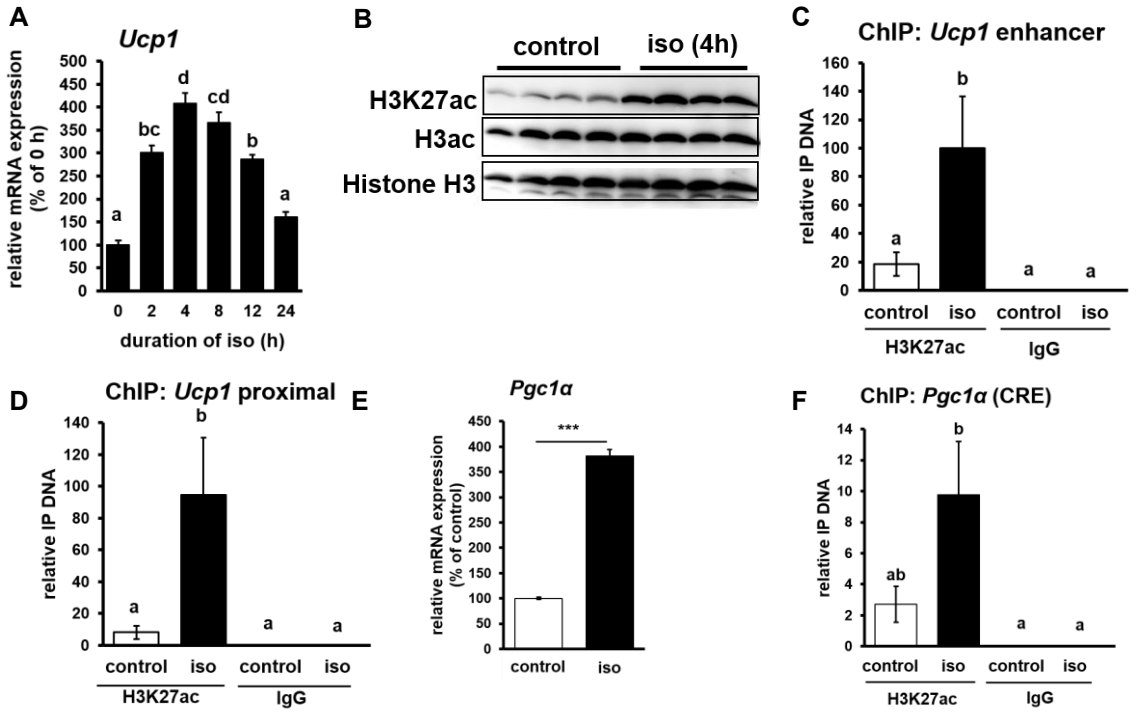

Figure 4. Histone acetylation state under β-adrenergic receptor (β-AR) stimulation in IWAT cells. (**A**) *Ucp1* expression after induction by 10 μM β-AR agonist isoproterenol (iso) over time, and H3K27ac level in (**B**) whole cells, (**C**) *Ucp1* enhancer region, and (**D**) *Ucp1* proximal region after induction by 10 μM iso for 4 h. (**E**) Peroxisome proliferator-activated (PPAR) gamma coactivator 1-alpha (*Pgc1α*) and (**F**) H3K27ac level in *Pgc1α* cAMP response element (CRE) region in IWAT cells after trated with 10 μM iso for 4 h. IgG act as a mock control. Data are presented as mean ± S.E.M. (error bars). n = 4–6 in each group. Different letters indicate significant difference ($p < 0.05$) according to one-way ANOVA followed by the Tukey-Kramer multiple comparison test. Same letters indicate non-significant difference. *** indicates significant difference ($p < 0.001$) according to unpaired-t test.

β-AR-stimulated *Ucp1* transcriptional activation is associated with inhibition of class I but not class II HDAC in IWAT cells

After confirming favorable chromatin state for *Ucp1* expression during β-AR stimulation, we investigated the role of HDAC, one of the main regulators of histone acetylation. HDAC activity was suppressed under isoproterenol induction (Figure 5A), displaying the opposite pattern to the level of *Ucp1* measured in the time-course experiment (Figure 4A). These data established a negative correlation between *Ucp1* and HDAC activity. To investigate the regulation behind HDAC inhibitory activity, we first examined the mRNA level of class I and II HDACs, as HDIs, which previously reported to induce browning, mainly inhibit these two classes [32,42,43]. Almost all class I HDAC mRNAs, except *Hdac2*, were suppressed significantly upon isoproterenol treatment (Figure 5B–E, left side). In addition, Pearson's correlation showed a strong negative correlation between class I HDAC mRNAs and *Ucp1* expression (Figure 5B–E, right side), which was consistent with the result from the measurement of HDAC activity (Figure 5A). On the contrary, class II HDAC mRNAs were barely altered and showed weaker correlation with *Ucp1* (Figure 5F–H). These results accentuate the importance of class I HDAC specificity, as confirmed by the remarkable increase of *Ucp1* expression after treatment with the class I HDAC inhibitor MS275 (Figure 6A), while also significantly decreasing HDAC activity (Figure 6B) in IWAT cells. Yet, among class I HDAC, *Hdac3* and *Hdac8* showed the highest correlation with *Ucp1* (Figure 5D,E right side), while *Hdac1* and *Hdac7* showed a relatively good correlation (Figure 5B, G right side).

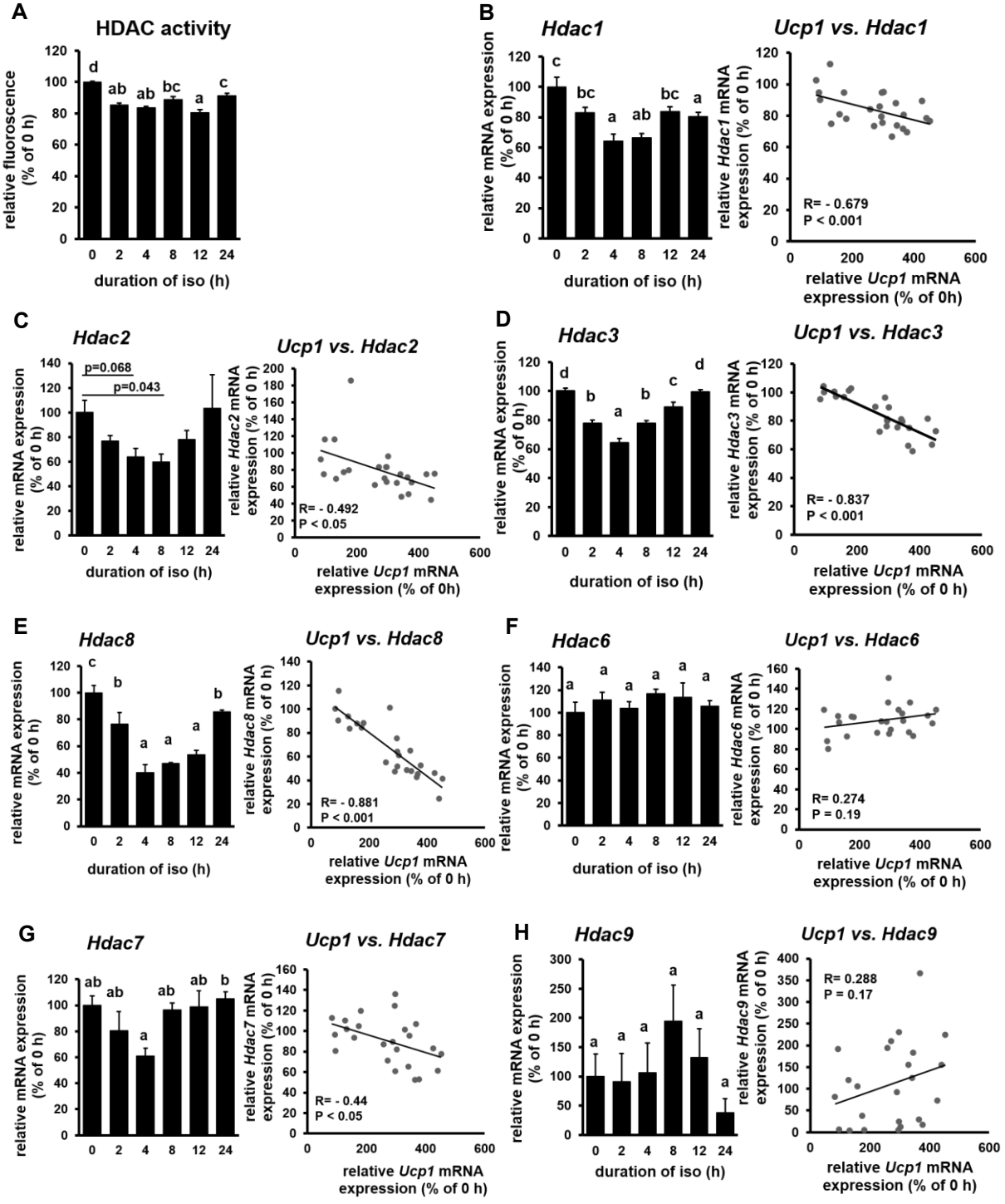

Figure 5. β-AR stimulation regulates histone deacetylase (HDAC) expression in IWAT cells. (**A**) HDAC activity, class I HDAC mRNA: (**B**) *Hdac1*, (**C**) *Hdac2*, (**D**) *Hdac3*, and (**E**) *Hdac8*; and class II HDAC mRNA: (**F**) *Hdac6*, (**G**) *Hdac7*, and (**H**) *Hdac9* expression after induction by 10 μM iso in a time-course experiment. HDAC mRNA expression (left side) and its association with *Ucp1* (right side) based on Pearson's correlation. Data are presented as mean ± S.E.M. (error bars). n = 4–8 in each group. Different letters indicate significant differences ($p < 0.05$) according to one-way ANOVA followed by the Tukey-Kramer multiple comparison test. Same letters indicate non-significant difference.

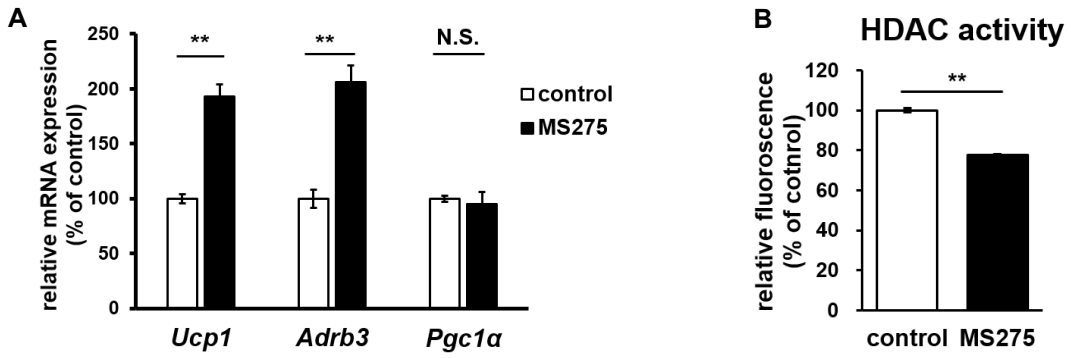

Figure 6. Class I HDAC inhibitor MS275 regulation on *Ucp1* expression in IWAT cells.
(**A**) Browning-related genes expression and (**B**) HDAC activity after treated with 0.15 μM MS275 for 24 h. Data are presented as mean ± S.E.M. (error bars). n = 4–8 in each group. ** indicates significant difference ($p < 0.01$) according to unpaired-t test. N.S., not significant.

HDAC1, HDAC7, and HDAC8 might not be involved in *Ucp1* regulation in IWAT cells

Of the two best candidates of genes for *Ucp1* regulation, *Hdac3* and *Hdac8*, we first investigated the specific role of *Hdac8*. Initially, IWAT cells were transfected with *Hdac8* siRNA to mimic *Hdac8* downregulation, followed by isoproterenol treatment, and *Ucp1* expression was measured. However, *Hdac8* siRNA interference failed to improve *Ucp1* expression, both on a basal level (Figure 7A) or under isoproterenol stimulation (Figure 7B). During isoproterenol induction, although *Hdac8* mRNA was downregulated (Figure 5E, left side), HDAC8 protein level was barely changed (Figure 7C), which might explain why *Ucp1* expression was unaffected by *Hdac8* siRNA.

Previous reports have shown that HDAC8 activity is highly regulated through post-translational modification by phosphorylation, mediated by protein kinase A (PKA) [44,45], which is activated in β-AR stimulation [12]. Phosphorylation of HDAC8 resulted in a decrease of HDAC8 activity [44], which was shown upon isoproterenol treatment of IWAT cells (Figure 7C), and this was further altered by PKA inhibition by H89. However, as HDAC8 activity was reduced, rescuing its activity by adding the HDAC8 coactivator TM251 barely altered *Ucp1* expression (Figure 7D, E). Additionally, IWAT cells were also treated with the selective HDAC8 inhibitor,

PCI34051, under isoproterenol induction. Yet, we observed no significant change in *Ucp1* expression (Figure 7F,G). These data suggest that HDAC8 might not be involved in promoting *Ucp1* expression during β-AR stimulation.

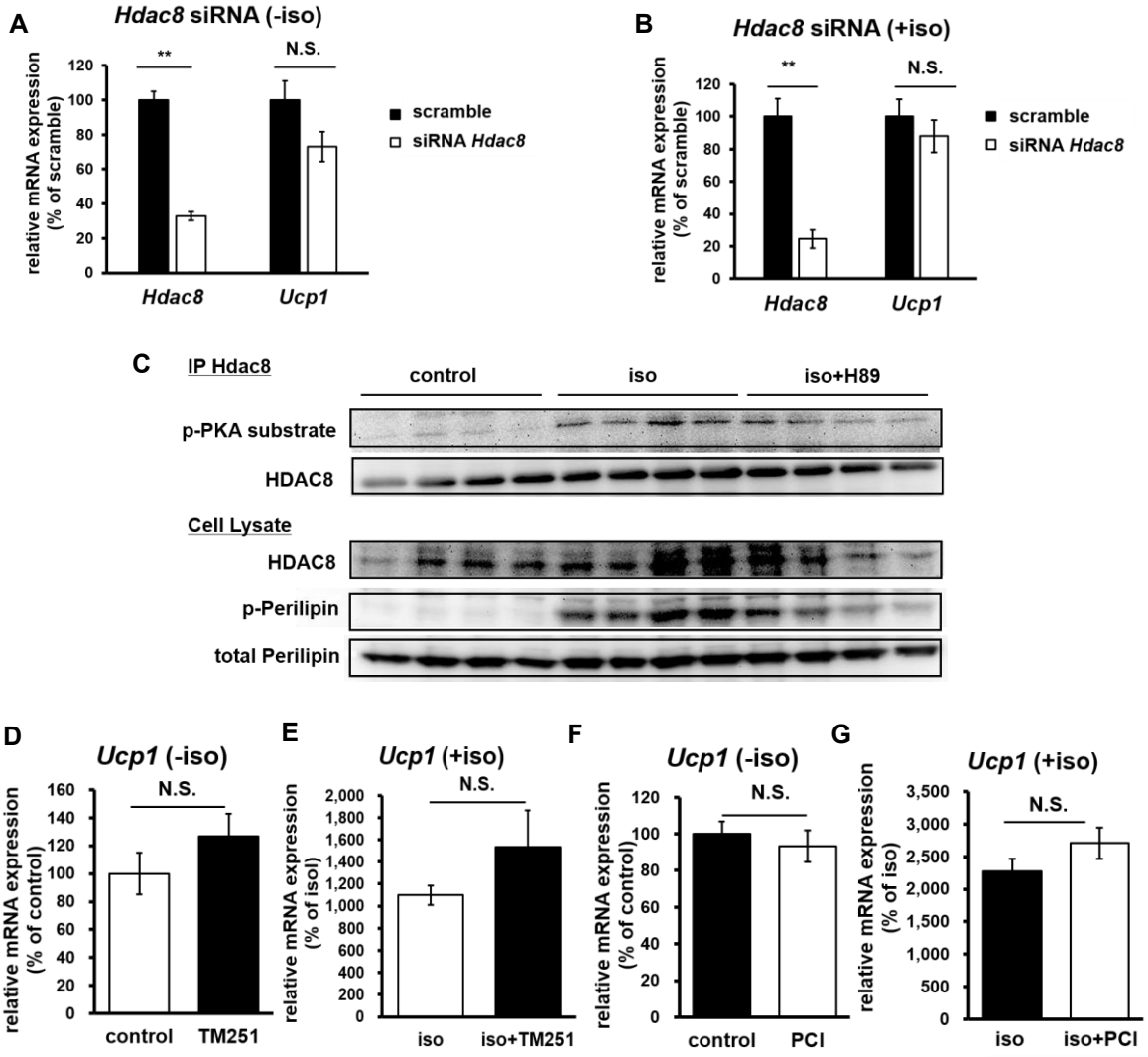

Figure 7. HDAC8 modification has no effect on *Ucp1* regulation in IWAT cells.

Hdac8 and *Ucp1* expression after transfection with *Hdac8* siRNA for 24 h without (**A**) or with (**B**) 10 μM iso induction for 2 h. (**C**) Protein kinase A (PKA) phosphorylation of immunoprecipitated HDAC8 after induced by 10 μM iso or pre-incubated with 5 μM PKA inhibitor (H89) for 4.5 h (iso was added in the last 4 h of H89 incubation). *Ucp1* expression after treatment with 20 μM HDAC8 activator TM251 without (**D**) or with (**E**) 10 μM iso induction for 4 h. *Ucp1* expression after treatment with 5 μM HDAC8 inhibitor PCI34051 (PCI) for 24 h without (**F**) or with (**G**) 10 μM iso induction at the last 4 h. Data are presented as mean ± S.E.M. (error bars). n = 4–6 in each group. ** indicates significant difference ($p < 0.01$) according to unpaired-t test. N.S., not significant.

Similar to HDAC8, the decrease in *Hdac1* and *Hdac7* mRNA level, which have shown a relatively good correlation with *Ucp1* expression, were not followed by their protein level. HDAC1 and HDAC7 protein level were barely changed under isoproterenol treatment (Figure 8A, B), suggesting HDAC1 and HDAC7 were not likely to contribute to the regulation of *Ucp1* expression during β-AR stimulation.

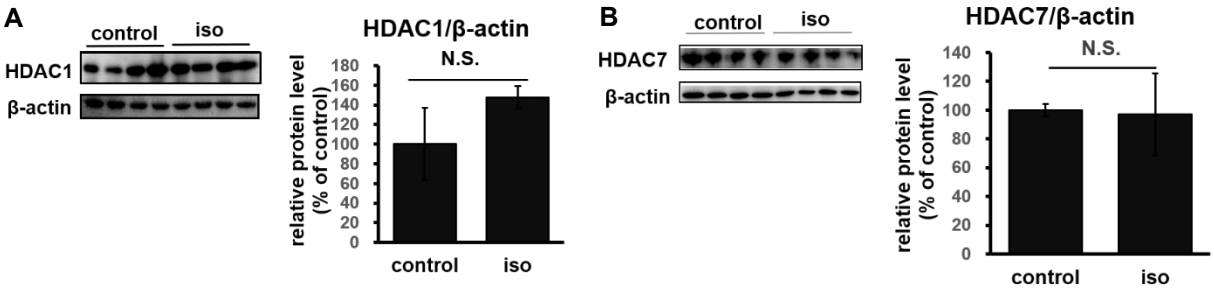

Figure 8. HDAC1 and HDAC7 protein level under β-AR stimulation in IWAT cells.
(**A**) HDAC1 and (**B**) HDAC7 protein level after induced by 10 μM iso. Protein quantification by ImageJ. Data are presented as mean ± S.E.M. (error bars). n = 4 in each group. N.S. indicate not significant according to unpaired-t test.

HDAC3 inhibition plays a major role in *Ucp1* transcriptional activation during β-AR stimulation in IWAT cells

When IWAT cells were treated with isoproterenol, *Hdac3* mRNA was significantly downregulated (Figure 5D, left side). Consistently, the level of HDAC3 protein was also reduced (Figure 9A). We investigated whether this decrease in HDAC3 protein level affected HDAC3 recruitment to the *Ucp1* enhancer region at the same site of induced histone activation mark H3K27ac, as shown in Figure 4C. The results showed that the HDAC3 recruitment level in the *Ucp1* enhancer region (Figure 9B) was inhibited significantly after isoproterenol addition.

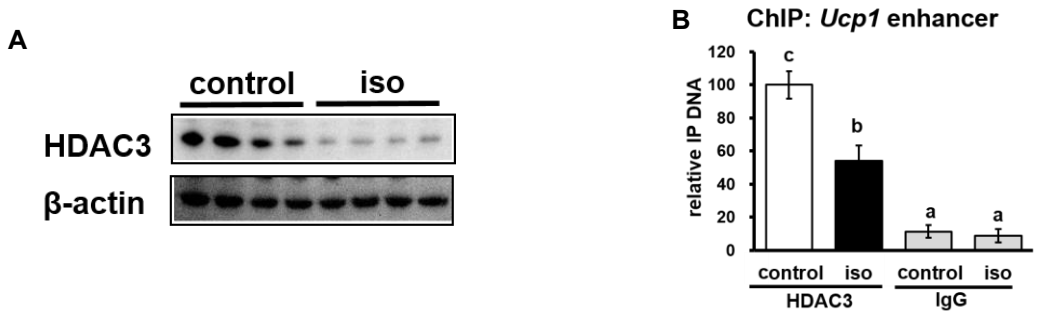

Figure 9. HDAC3 protein level was decreased under β-AR stimulation in IWAT cells.
(**A**) HDAC3 protein level, and its recruitment level in (**B**) the *Ucp1* enhancer region after treatment with 10 μM iso for 4 h. Data are presented as mean ± S.E.M. (error bars). n = 4–6 in each group. β-actin act as loading control and IgG as a mock control. Different letters indicate significant differences ($p < 0.05$) according to one-way ANOVA followed by the Tukey-Kramer multiple comparison test. Same letters indicate non-significant difference.

Next, to specifically examine the role of *Hdac3* mRNA downregulation on *Ucp1* expression, *Hdac3* expression was interrupted by transfecting *Hdac3* siRNA into IWAT cells. Although not at the basal level (Figure 10A), *Hdac3* siRNA successfully increased *Ucp1* expression under isoproterenol stimulation (Figure 10B). Next, to further confirm the significance of HDAC3-specific inhibition of histone acetylation and *Ucp1* regulation, a selective inhibitor of HDAC3 (RGFP966) was used in IWAT cells. HDAC3 inhibitor treatment showed a significant decrease in HDAC activity (Figure 10C) and escalated H3K27 acetylation (Figure 10D). Unlike *Hdac3* siRNA, HDAC3 inhibitor alone was sufficient to induce *Ucp1* expression even at the basal level (Figure 10E), while also successfully enhancing *Ucp1* under isoproterenol induction (Figure 10F). Interestingly, neither adrenoceptor beta 3 (*Adrb3*), nor several influential coactivators of *Ucp1*, such as *Pgc1a*, *Ppara*, and *Pparγ* benefitted upon HDAC3 inhibition (Figure 10E,F), although class I HDAC inhibition by MS275 significantly upregulated *Adrb3* (Figure 6A). These results suggest that HDAC3 might be specifically and directly involved in *Ucp1* upregulation during β-AR stimulation.

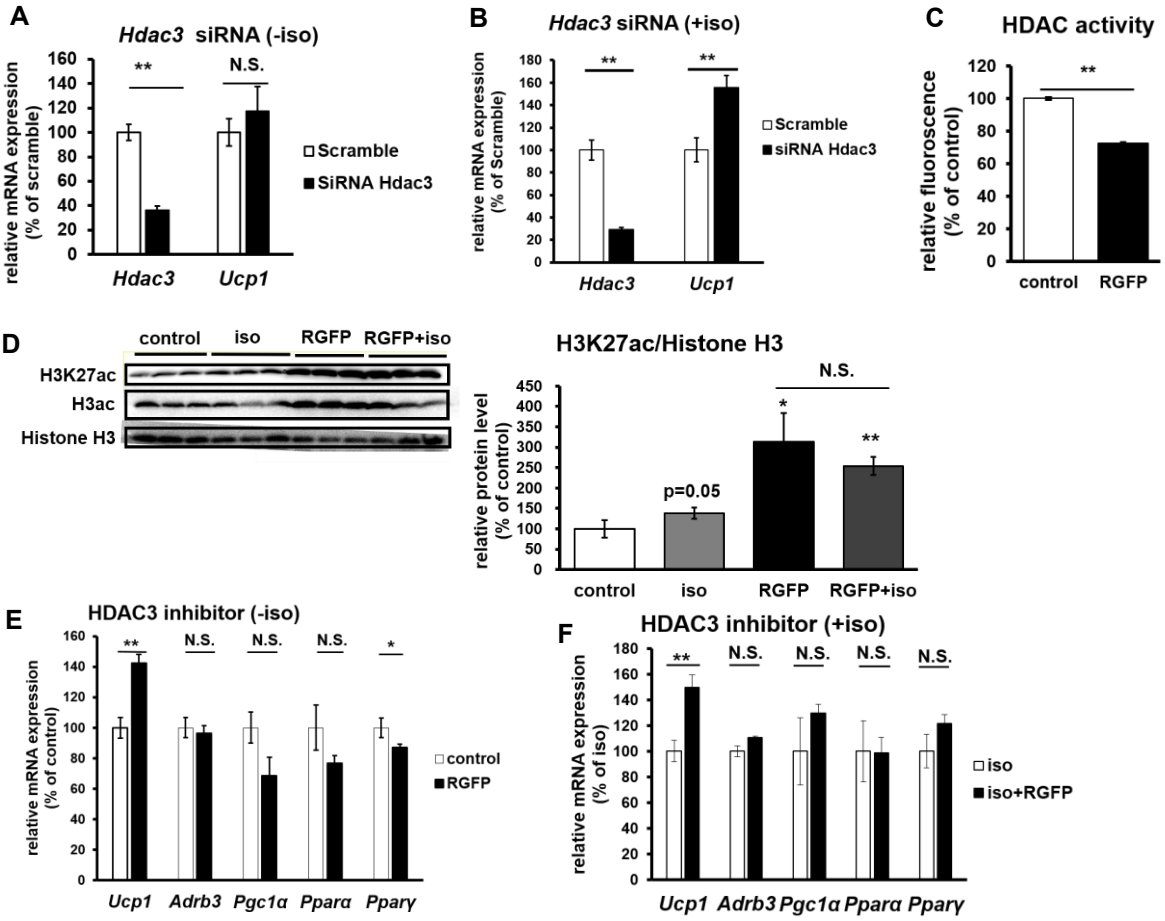

Figure 10. HDAC3 inhibition resulted in *Ucp1* upregulation in IWAT cells.

Hdac3 and *Ucp1* expression after transfection with *Hdac3* siRNA for 24 h without (**A**) or with (**B**) 10 μM iso induction for 2 h. (**C**) HDAC activity after treatment with HDAC3 inhibitor RGFP966 (RGFP) for 24 h. (**D**) H3K27ac level after induction by 10 μM iso for 4 h, 5 μM RGFP for 24 h, or both compounds. Protein band were quantified by ImageJ. Browning-related gene expression after treatment with 5 μM RGFP for 24 h without (**E**) or with (**F**) 10 μM iso induction in the last 4 h. Data are presented as mean ± S.E.M. (error bars). n = 3–6 in each group. *, ** indicate significant differences at $p < 0.05$ and $p < 0.01$, respectively, according to unpaired-t test. N.S., not significant.

Discussion

The favourable open chromatin structure for *Ucp1* transcriptional activation after β-AR stimulation has been previously reported in cultured brown adipocytes, demonstrated by a significant increase of H3K27ac in both the *Ucp1* and *Pgc1a* promoter regions [27]. However, which factors regulate behind this phenomenon is still unclear. The potential of HDAC, as one of

the main regulators of histone acetylation, to regulate browning in adipose tissue has been suggested by several studies that tested HDAC inhibitory compounds in both BAT and WAT [26,34,38]. Moreover, many HDIs have shown to be beneficial in alleviating obesity and various diseases [34–37,46–50]. All of these reports suggest the possibility of β-AR activation to also possess HDAC inhibitory activity, which could explain the escalated H3K27ac phenomenon under this stimulation. Indeed, we showed for the first time that HDAC was inhibited during β-AR stimulation in beige adipocytes (IWAT cells) and thus played an active role in *Ucp1* regulation, notably through HDAC3. HDAC3 was consistently suppressed at both the mRNA and protein level, which resulted in the lower HDAC3 recruitment to the *Ucp1* enhancer region. The reduced HDAC3 recruitment thus directly cause an increased acetylation of H3K27 in the same site of *Ucp1* enhancer region and promote *Ucp1* transcriptional activation, as shown in this study. The *Ucp1* enhancer region (~2631–2343 bp upstream) is known as the PPAR response element (PPRE) coactivated by PGC1α [8,51]. The suppression of HDAC3 in this region might promote PGC1α coactivator complex binding to the *Ucp1* enhancer and thus activate *Ucp1* transcription.

Interestingly, *Hdac3* interference by siRNA did not result in *Ucp1* upregulation at the basal level, but improved *Ucp1* expression under isoproterenol stimulation, suggesting that *Hdac3*-regulated *Ucp1* transcriptional activation is dependent on β-AR stimulation. HDAC3 inhibitor treatment successfully enhanced *Ucp1* expression in both conditions. HDI decrease HDAC activity by disrupting the formation of the HDAC corepressor complex and hence it failed to be recruited to chromatin [52]. The same mechanism similarly happened to HDAC3 recruitment level to *Ucp1* promoter when stimulated with isoproterenol, as shown in this report. Thus, the reduction of HDAC3 recruitment level to the chromatin is important for *Ucp1* transcriptional activation, as its loss greatly affected histone acetylation state. HDAC3 might also specifically regulate *Ucp1* expression, because the treatment of HDAC3 inhibitor barely altered the mRNA expression of other browning markers such as *Adrb3*, *Pgc1a*, *Ppara*, and *Pparγ*. On the other

hand, pan-HDAC inhibitor [34] or class I HDAC inhibitor MS275 [38] was shown to upregulate not only *Ucp1*, but also *Adrb3* mRNA expression and other browning-related markers.

A previous report has shown that HDAC3-deficient mice underwent significant re-modelling of the WAT metabolic pathway to resemble BAT (browning) without β-AR stimulation [28]. This study thus highlights a negative regulation of HDAC3 to WAT browning. However, the reason why loss of HDAC3 was capable to induce browning remains unclear. Accordingly, our study clarifies the outcome of WAT browning in HDAC3 deficient mice might be because it has the same effect of HDAC3 suppression originated from β-AR stimulation to regulate *Ucp1* expression. Interestingly, the other study showed that the ablation of HDAC3 in mice during cold exposure (4 °C, 24 h) failed to activate the thermogenesis program in BAT [53]. In contrast, this study suggests a positive regulation of HDAC3 to browning. The different reports raise a question regarding the positive or negative role of HDAC3 in browning. To address the issue of the opposite role of HDAC3, in our preliminary study we found that H3K27ac was also differentially regulated during initial and chronic stage of cold exposure. The level of H3K27ac increased at the initial stage of cold challenge (0–24 h, 10 °C) but decreased after long exposure (48–96 h, 10 °C), although *Ucp1* expression was stably increased (data not shown). We thus suggest that the opposite HDAC3 regulation in browning might associate with a different regulation of H3K27ac during initial and chronic stage of cold exposure. Our in vitro study matched the initial stage of H3K27ac of cold stimulation in vivo. In the initial stage of cold exposure, the regulation of histone acetylation could be important for inducing *Ucp1* expression, as several studies [26,28], including this report, have suggested. Further research is needed to confirm the regulation of HDAC3 and H3K37ac in relation to *Ucp1* expression during chronic cold exposure.

Besides *Hdac3*, *Hdac1*, *Hdac7*, and *Hdac8* mRNA also showed a good association with *Ucp1* expression. However, HDAC1 and HDAC7 protein level were barely changed under isoproterenol treatment. In addition, HDAC1 specific inhibitor showed a negative effect on *Ucp1*

expression. (data not shown). Although HDAC1 deficiency has been reported to be involved in regulating BAT activation [27], it might be regulated differentially in beige adipocytes, as seen in this study. The role of HDAC1 in WAT browning, especially in beige adipocytes, should be confirmed in the future. Interestingly, isoproterenol treatment clearly mediated phosphorylation of HDAC8 through PKA, which has been established to decrease HDAC8 activity and resulted in hyperacetylation of histone H3 and H4 or non-histone protein [44]. It is also known that protein kinase A (PKA) is stimulated during β-AR stimulation, which resulted in the induction of *Ucp1* expression [7,12,21,54,55]. However, we found that HDAC8 might not be involved directly in *Ucp1* regulation. Additional research is needed to investigate the consequences of HDAC8 downregulation, particularly on non-histone substrates. Apart from 3600 possible acetylation sites (which served as HDAC substrate) that have been identified, 1750 site are non-histone protein [43,56–59]. Although we have demonstrated the HDAC inhibition in mediating acetylation of histone H3K27, the possibility of HDAC to also induce acetylation of non-histone substrate and their subsequent effect cannot be ruled out completely.

Several pan-HDAC inhibitors have been approved for drug use and more HDAC inhibitors are under clinical trials, intended for cancer treatment [60]. Proportionally, HDAC inhibitor-based therapies have been recognized to be applicable to treat human disease. However, there is a concern over the side effects of pan-HDAC inhibitor [61], shifting the interest to more specific HDAC target. To address this issue, our study showed HDAC3 as a potential, more specific target for WAT browning. Many studies have also concluded HDAC3 as an emerging target for inflammation, insulin-resistance, and type 2 diabetes [48,62–66] which are closely related to obesity. Future study might be directed to the capability of the HDAC3 inhibitor to induce browning of WAT, as our study highly suggested, especially in humans. It has been known that browning of WAT has been targeted not only to treat obesity, but also related metabolic disorders including insulin resistance, inflammation, and type-2 diabetes. Accordingly, our study added a

solid background of the HDAC3 hidden potential in regulating *Ucp1* expression under β-AR stimulation.

Chapter 2

Endoplasmic reticulum stress impaired uncoupling protein 1 expression via the suppression of peroxisome proliferator-activated receptor γ transcriptional activity[2]

Introduction

Adipose tissue has been broadly characterized as white and brown adipocytes through their distinct characteristics in lipid metabolism. White adipose tissue (WAT) functions as energy storage, while brown adipose tissue (BAT) dissipates energy as heat supported by its high oxidative capacity [4,7,8]. Recent findings show inducible brown-like white adipocytes, known as beige adipocytes. Beige adipocytes are developed within WAT in response to β-adrenergic receptor (β-AR) stimulation, termed as browning of WAT, and exhibit similar characteristic as BAT [7,67].The transcription of uncoupling protein 1 (*Ucp1*) is tightly regulated during browning, thus it is often used as a browning marker of adipose tissue [8,13]. Interestingly, in addition to browning, beige adipocytes also show unique plasticity to undergo whitening (reversal of browning) [68–70].

The endoplasmic reticulum (ER) is a critical organelle in sensing and handling cellular nutrient required for normal cellular functions and survival [71]. Certain physiological and pathological factors such as nutrient deprivation, lipids, or increased synthesis of secretory proteins can induce cell stress and disrupt ER homeostasis by promoting unfolded protein overload [71]. Unfolded protein response (UPR) is activated as an adaptive response to restore

[2] The content described in this chapter was originally published in International Journal of Molecular Sciences (IJMS). Yuliana A, Daijo A, Jheng HF, Kwon J, Nomura W, Takahashi H, Ara T, Kawada T, and Goto T. Endoplasmic Reticulum Stress Impaired Uncoupling Protein 1 Expression via the Suppression of Peroxisome Proliferator-Activated Receptor γ Binding Activity in Mice Beige Adipocytes. Int. J. Mol. Sci. (2019), 20(2):274, 1-15. doi: 10.3390/ijms20020274

ER activity and maintain protein quality to ensure proper protein synthesis, secretion, and correct folding of protein [20,72,73]. When ER stress is severe and/or prolonged, it can shift toward apoptosis (cell death), although the mechanism for this transition is not well understood [72,74–76]. ER stress has been linked to multiple disorders ranging from neurodegenerative diseases to metabolic disorders such as obesity, insulin resistance, type 2 diabetes, and chronic inflammation [71,72,77]. Metabolically active tissue including adipose tissue is not excluded from the ER stress outcomes [78–80]. However, the consequences of ER stress on adipocyte functions including thermogenic capacity are poorly understood.

In adipose tissue, obesity results in chronic stress and dysfunction caused by the increased demand of synthetic machinery [78]. Several studies have shown a significant activation of ER stress in high-fat-induced obesity [19,81,82]. In addition, both brown and beige adipocytes activation stimulated by cold exposure was impaired in obese adipose tissue [83]. Adversely, a decrease in adaptive thermogenesis has also been suggested as a contributing factor to obesity [68]. As obesity is characterized by diverse metabolic symptoms such as ER stress and inflammation, there is still no direct link about how ER stress itself could regulate *Ucp1* expression in beige adipocytes. Previous study has shown that the activation of downstream signaling in ER stress, such as that involving inositol-requiring enzyme 1α (IRE1α) and X-box binding protein 1 (XBP1), was needed for *Ucp1* expression in BAT [77]. Further, the inactivation of ER stress in BAT, WAT, or macrophages resulted in an improved adaptive thermogenesis response [68,84], while treatment of chemical chaperones (ER stress inhibitor) could increase energy expenditure and activate browning of WAT [85–87]. These reports suggest a possible unknown regulatory mechanism of ER stress in the browning of WAT. In this study, we investigated the effect of ER stress stimulation on *Ucp1*, an adipocyte browning marker, in beige adipocytes.

Material and methods

Materials

All chemicals were obtained from Nacalai Tesque (Kyoto, Japan), Wako (Osaka, Japan), Corning (Corning, NY, USA), Qiagen (Hilden, Germany), Invitrogen (Carlsbad, CA, USA), and Sigma-Aldrich (St. Louis, MO, USA). Tunicamycin, U0126, SP600125, and cycloheximide were purchased from Nacalai Tesque (Kyoto, Japan). GW9662 (Sigma-Aldrich, St. Louis, MO, USA), rosiglitazone (LKT Laboratories, St. Paul, MN, USA), and PBA (Santa Cruz Biotechnology, Dallas, TX, USA) were acquired from the indicated companies.

Animal experiment

Mice were kept in a temperature-controlled room at 23 ± 1 °C with a 12 h light/dark cycle and free access to food (standard diet) and water. To stimulate browning, 6–10-week-old male C57BL/6J mice (SLC, Shizuoka, Japan) were intraperitoneally injected with 10 mg/kg rosiglitazone daily for 10 days [88]. On day 10, 10 mg/kg tunicamycin was injected to induce ER stress. Mice were then fasted overnight. Twenty-four hours after the last injection, mice were sacrificed, and IWAT was harvested for mRNA and protein analysis. The mice were handled in accordance with procedures approved by the Kyoto University Animal Care Committee (Permission number: 29-62, 20 April 2012).

Ex vivo experiment

To stimulate browning, 6-week-old male C57BL/6J mice (SLC, Shizuoka, Japan) were intraperitoneally injected with 10 mg/kg rosiglitazone daily for 10 days [88]. Twenty-four hours after last injection, IWAT was collected and immediately incubated in serum free medium containing 1 μM tunicamycin for 24 h with or without 100 μM extracellular signal-regulated kinase (ERK) inhibitor (U0126) for 26 h / 25 μM c-Jun N-terminal kinase (JNK) inhibitor (SP600125) for 25 h. IWAT was then extracted for mRNA analysis.

Cell culture

Immortalized primary inguinal white adipose tissue (IWAT) cells were kindly provided by Dr. S. Kajimura (University of California, San Francisco, CA, USA). IWAT cells were maintained in a humidified 5% CO2 atmosphere at 37 °C using basic medium (DMEM) supplemented with 10% fetal bovine serum and 1% penicillin/streptomycin. To induce the differentiation into beige adipocytes [88], two days post-confluent IWAT cells were stimulated with 0.5 mM 1-methyl-3-isobutylxanthine, 2 μg/mL dexamethasone, 10 μg/mL insulin, 1 nM triiodo-L-thyronine (T3), 0.5 μM rosiglitazone (rosi), and 125 μM indomethacin for 48 h. The media was then replaced by basic medium containing 5 μg/mL insulin, 1 nM T3, and 0.5 μM rosi every 2 days. Generally, the differentiation process took 8–10 days. ER stress was induced by the addition of tunicamycin (1 μM) in serum-free medium for 12 h, unless mentioned.

RNA preparation and quantification of gene expression

RNA was extracted as described previously [89]. Total RNA was collected from cultured cells or tissues using Sepasol-RNA I Super G (Nacalai Tesque, Kyoto, Japan) or QIAzol Lysis Reagent (Qiagen, Hilden, Germany), respectively. RNA expression was quantified by real-time PCR using a LightCycler System (Roche Diagnostics, Mannheim, Germany) with SYBR green fluorescence signal detection. All mRNA signals were normalized to a 36b4 internal control. The primer sequences are listed in Table 4.

Table 4. Primers used for RNA quantification

Gene	Forward	Reverse
Ucp1	5'-CAAAGTCCGCCTTCAGATCC-3'	5'-AGCCGGCTGAGATCTTGTTT-3'
Pparγ	5'-GGAGATCTCCAGTGATATCGACCA-3'	5'-ACGGCTTCTACGGATCGAAAACT-3'
36b4	5'-TCCTTCTTCCAGGCTTTGGG-3'	5'-GACACCCTCCAGAAAGCGAG-3'
Bip	5'-GTTTGCTGAGGAAGACAAAAAGCTC-3'	5'-CACTTCCATAGAGTTTGCTGATAAT-3'
Chop	5'-GTCCAGCTGGGAGCTGGAAG-3'	5'-CTGACTGGAATCTGGAGAG-3'

Protein extraction and western blotting

Western blotting was performed as previously described [89]. The protein concentration was measured using the DC protein assay (Bio-Rad, Hercules, CA, USA). The primary antibodies included anti-UCP1 (Sigma-Aldrich, St. Louis,MO, USA), anti-COXIV, anti-phospho-p44/42MAPK (ERK1/2), anti-phospho-SAPK/JNK (Thr183/Tyr185), anti-SAPK/JNK, anti-peroxisome proliferator-activated (PPAR) γ, and anti-β-actin (all purchased from Cell Signaling Technology, Danvers, MA, USA). The secondary antibody staining was visualized using a chemiluminescent horseradish peroxidase substrate (Millipore, Burlington, MA USA).

Chromatin immunoprecipitation (ChIP) assay

The ChIP assay was performed as described previously [89]. The cells were subjected to overnight immunoprecipitation with 8 μg PPARγ antibody (Perseus Proteomics, Tokyo, Japan), or rabbit IgG isotype control (Novus Biological, Littleton, CO, USA) as a mock control and analyzed by real-time PCR. The primer sequences are listed in Table 5.

Table 5. Primers used in ChIP assay

Gene	Forward	Reverse
Ucp1 enhancer	5'-CTCCTCTACAGCGTCACAGAGG-3'	5-AGTCTGAGGAAAGGGTTGA-3'

Luciferase assay

The luciferase assay was performed according to company protocol (Invitrogen, Carlsbad, CA, USA). Undifferentiated IWAT cells were transfected with plasmid containing the reporter vector driven by PPAR response element (PPRE-Luc) and a *Pparγ* expression vector using Lipofectamine 2000 reagent (Invitrogen, Carlsbad, CA, USA). The transfected cells were treated with 0.5 μM rosiglitazone for 24 h and 10 μM tunicamycin with or without 10 μM lactacystin for 4 h.

Statistical analysis

All data were analyzed using student's t-test or one-way ANOVA followed by Tukey–Kramer test, when variances were heterogeneous. All data are presented as means ± SEM. Differences were considered significant at $p < 0.05$.

Results

ER stress decreases *Ucp1* mRNA level in beige adipocytes

To investigate the regulation of ER stress on the thermogenic capacity of beige adipocytes, IWAT cells were differentiated to beige adipocytes and treated with tunicamycin, an ER stress inducer. ER stress stimulation was confirmed by the upregulation of ER stress markers: binding immunoglobulin protein (*Bip*) and CCAAT-enhancer-binding protein homologous protein (*Chop*) (Figure 11A). As mentioned before, chronic or prolonged ER stress could lead to the cell apoptosis. We found that our experimental condition showed an indication of cell apoptosis by the decrease in cell viability (Figure 11B) and increase in cleaved Caspase3 (Figure 11C). Consequently, *Ucp1* expression was severely suppressed (Figure 11A). The addition of chemical chaperone 4-phenylbutyrate (PBA) alleviated ER stress markers *Bip* and *Chop*, while also rescued *Ucp1* expression (Figure 11A). These results indicate that ER stress suppressed *Ucp1* expression in beige adipocytes.

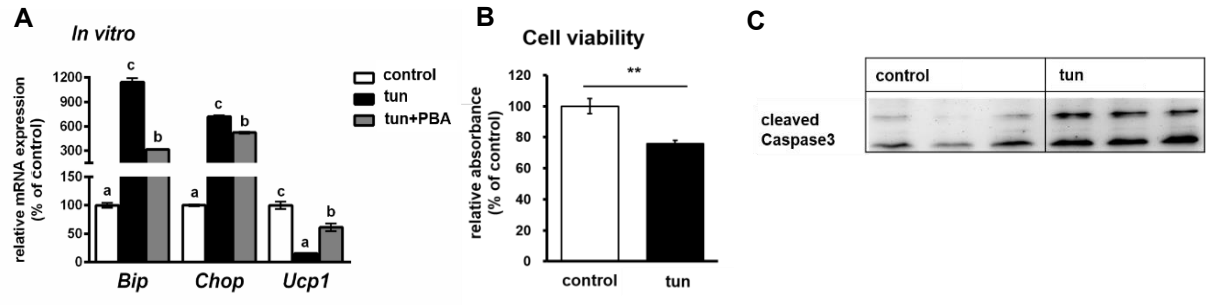

Figure 11. Endoplasmic reticulum (ER) stress stimulation downregulates uncoupling protein 1 (*Ucp1*) and induces cell apoptosis in inguinal white adipose tissue (IWAT) cells.

(**A**) The mRNA expression level of ER stress markers: binding immunoglobulin protein (*Bip*), CCAAT-enhancer-binding protein homologous protein (*Chop*), and adipocyte browning markers *Ucp1* after treatment with 1 μM tunicamycin (tun) for 12 h with or without 20 mM 4-phenylbutyrate (PBA) for 24 h before collection. (**B**) Cell viability of IWAT cells after treated with 1 μM tun for 12 h, analyzed by cell titer 96® Aqueous One Solution Cell Proliferation Assay (Promega, Madison, WI, USA). Cleaved Caspase3 protein level in (**C**) IWAT cells after treated with 1 μM tun for 12 h. Data are presented as mean ± S.E.M. (error bars). n = 3-5 each group. Different letters indicate significant differences ($p < 0.05$) according to one-way ANOVA followed by Tukey–Kramer multiple comparison test. ** indicates significant differences ($p < 0.01$) according to unpaired-t test.

Accumulating evidence has identified the cross-talk between UPR and the mitogen-activated protein kinase (MAPK) signaling pathway as a result of ER stress stimulation [74]. Indeed, we found ERK and JNK, which are parts of the MAPK signaling pathway, were activated by tunicamycin treatment in our experimental condition. Both ERK (Figure 12A) and JNK (Figure 12B) were phosphorylated after ER stress stimulation. The addition of either ERK or JNK inhibitor (U0126 or SP600125, respectively) could ameliorate tunicamycin-induced suppression of *Ucp1* expression (Figure 12C,D) while inhibiting the phosphorylation of ERK (Figure 12E) or JNK (Figure 12F), indicating an ER stress-induced suppression of *Ucp1* expression via the activation of ERK and JNK pathway.

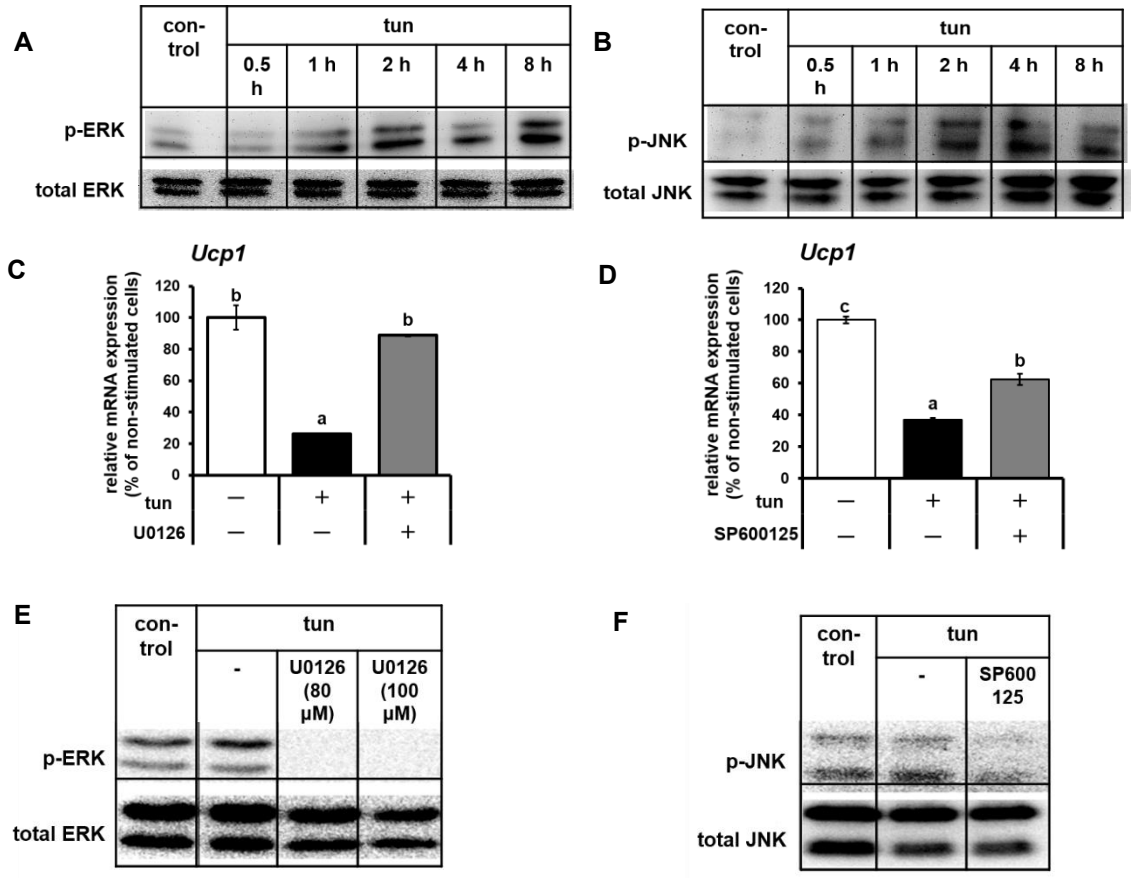

Figure 12. ER stress stimulation mediated the downregulation of *Ucp1* through the phosphorylation of extracellular signal-regulated kinase (ERK) and c-Jun N-terminal kinase (JNK) in IWAT cells. Phosphorylation of (**A**) ERK and (**B**) JNK at different time points when treated with 1 μM tun. (**C**,**D**) *Ucp1* mRNA expression and phosphorylation of ERK (**E**) or JNK (**F**) after being treated with (**C**,**E**) 80 or 100 μM ERK inhibitor (U0126) for 14 h, or (**D**,**F**) 25 μM JNK inhibitor (SP600125) for 13 h, followed by tun (1 μM; 12 h). Data are presented as mean ± S.E.M. (error bars). n = 4 in each group. Different letters indicate significant differences ($p < 0.05$) according to one-way ANOVA followed by Tukey–Kramer multiple comparison test.

ER stress induces downregulation of the *Ucp1* activator, PPARγ, preferably via the JNK pathway

It has been previously shown that PPARγ is a direct target of both ERK and JNK, which may result in decreased PPARγ transcriptional activity [90] and thus possibly affect *Ucp1* expression. Alongside *Ucp1* downregulation, the level of *Pparγ* mRNA was decreased upon tunicamycin treatment (Figure 13A,B) in IWAT cells but rescued when cells were treated with

either an ERK (Figure 13A) or JNK inhibitor (Figure 13B). Besides that, ER stress markers (*Bip*, *Chop* and spliced X-box binding protein 1 (*Xbp1s*)) were partially recovered through ERK and JNK inhibition (Figure 13C,D), indicating the involvement of ERK/JNK pathway in regulating *Pparγ* expression.

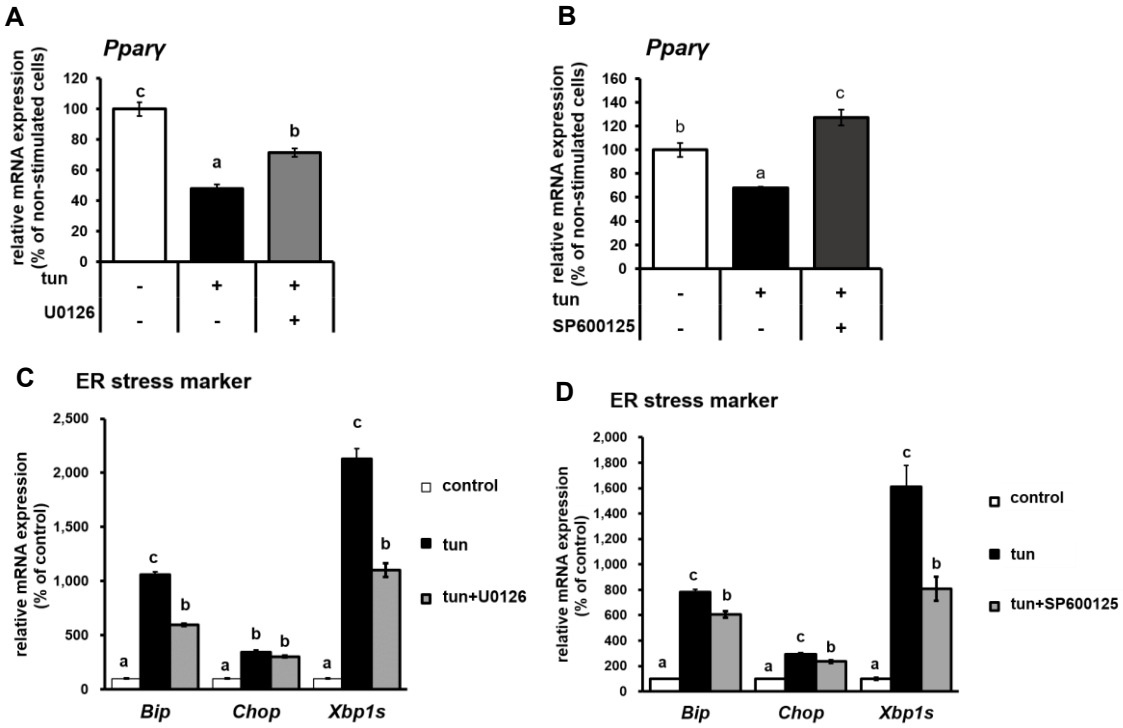

Figure 13. ER stress decreases *Ucp1* activator, peroxisome proliferator-activated receptor γ (*Pparγ*) mRNA expression through ERK and JNK pathway in IWAT cells.

Pparγ and ER stress marker (*Bip*, *Chop*, and spliced X-box binding protein 1-*Xbp1s*) mRNA expression in cells treated with (**A**,**C**) 100 μM U0126 for 14 h or (**B**,**D**) 25 μM SP600125 for 13 h, followed by tun (1 μM, 12 h). Data are presented as mean ± S.E.M. (error bars). n = 4 in each group. Different letters indicate significant differences ($p < 0.05$) according to one-way ANOVA followed by Tukey–Kramer multiple comparison test.

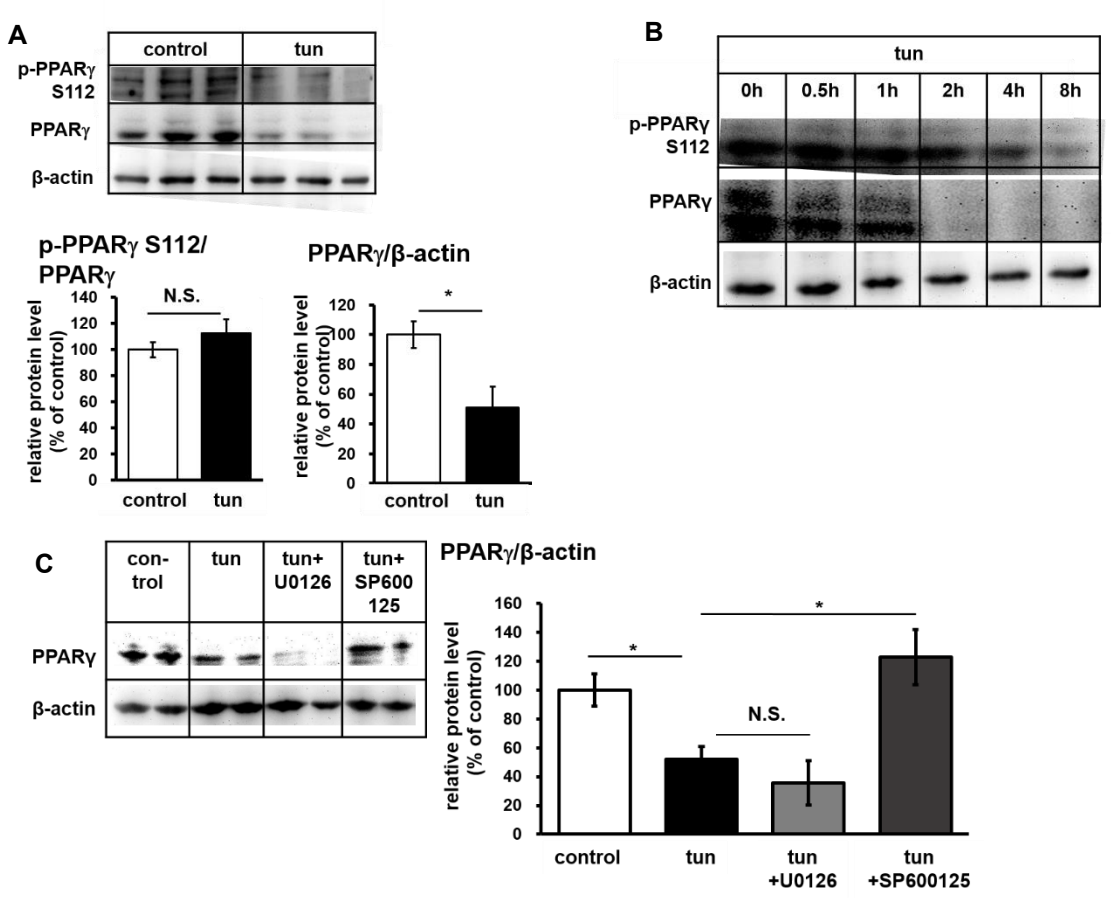

Figure 14. ER stress decreases PPARγ protein level preferably through JNK pathway in IWAT cells. PPARγ phosphorylation at serine 112 (S112) and PPARγ protein level in cells treated with 1 μM tunicamycin (**A**) for 12 h or (**B**) at different time points. (**C**) PPARγ protein after treated with 100 μM U0126 for 14 h or 25 μM SP600125 for 13 h, followed by tun (1 μM, 12 h). β-actin was used as a loading control. Data are presented as mean ± S.E.M. (error bars). n = 3–4 in each group. * indicates significantdifferences ($p < 0.05$) according to unpaired-t test. N.S., not significant.

We further investigated the possibility of post-translational modifications of PPARγ through the phosphorylation in serine 112 (S112), which is one of the main targets of ERK/JNK [91]. However, we did not find any change in the level of phosphorylation; instead, the PPARγ protein level was significantly reduced (Figure 14A). A time-course experiment revealed that the decrease in the PPARγ protein level was initiated earlier than the decrease in phosphorylation of PPARγ at S112 (Figure 14B). At this time (~4 h), ERK and JNK were both activated (Figure

12B,C). However, only treatment with the JNK inhibitor, but not the ERK inhibitor, could rescue PPARγ protein level (Figure 14C), suggesting that JNK is the main pathway for the tunicamycin-induced reduction in PPARγ protein.

Next, to confirm the role of PPARγ in ER stress-regulated *Ucp1* expression, we treated IWAT cells with PPARγ antagonist (GW9662). GW9662 similarly decreased *Ucp1* expression as tunicamycin (Figure 15A,B). However, the addition of GW9662 in tunicamycin treatment did not enhance the suppression of *Ucp1* expression (Figure 15A,B), suggesting that ER stress-suppressed *Ucp1* expression is indeed mediated through PPARγ.

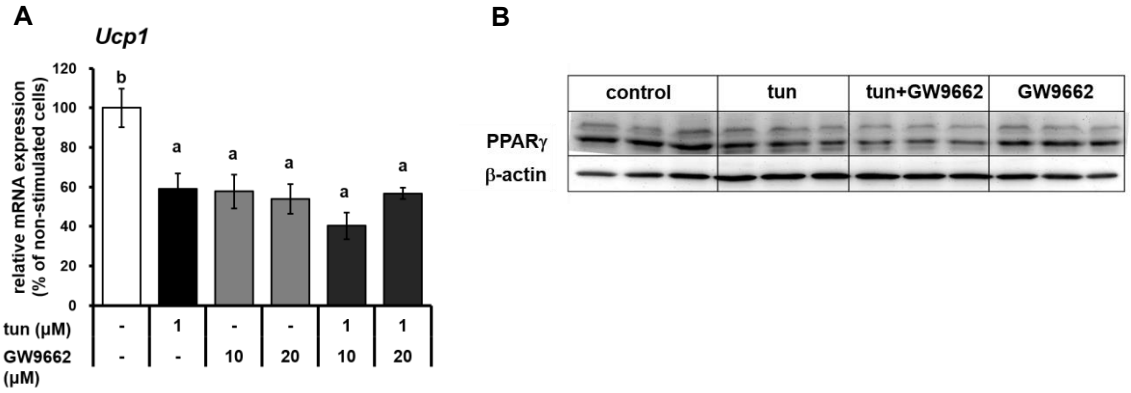

Figure 15. ER stress suppressed *Ucp1* expression through the reduce activity of PPARγ in IWAT cells. (**A**) *Ucp1* mRNA expression and (**B**) PPARγ protein level after treatment with 10 μM or 20 μM PPARγ antagonist (GW9662) for 13 h, followed by tun (1 μM, 12 h). β-actin was used as a loading control. Data are presented as mean ± S.E.M. (error bars). n = 4 in each group. Different letters indicate significant differences ($p < 0.05$) according to one-way ANOVA followed by Tukey–Kramer multiple comparison test.

ER stress stimulates PPARγ degradation that leads to the reduced binding activity

Next, to investigate whether the decreased PPARγ protein was dependent on the decrease in its mRNA expression, we performed a cycloheximide chase experiment to measure PPARγ protein stability. Tunicamycin treatment seemed to accelerate PPARγ degradation under cycloheximide addition (Figure 16A). The half-life of PPARγ was significantly reduced from 5.9 to 3.5 h upon tunicamycin treatment (Figure 16B). However, the addition of proteasome inhibitor

(lactacystin) could rescue PPARγ protein (Figure 16C), suggesting that the degradation of PPARγ was mediated via proteasome degradation.

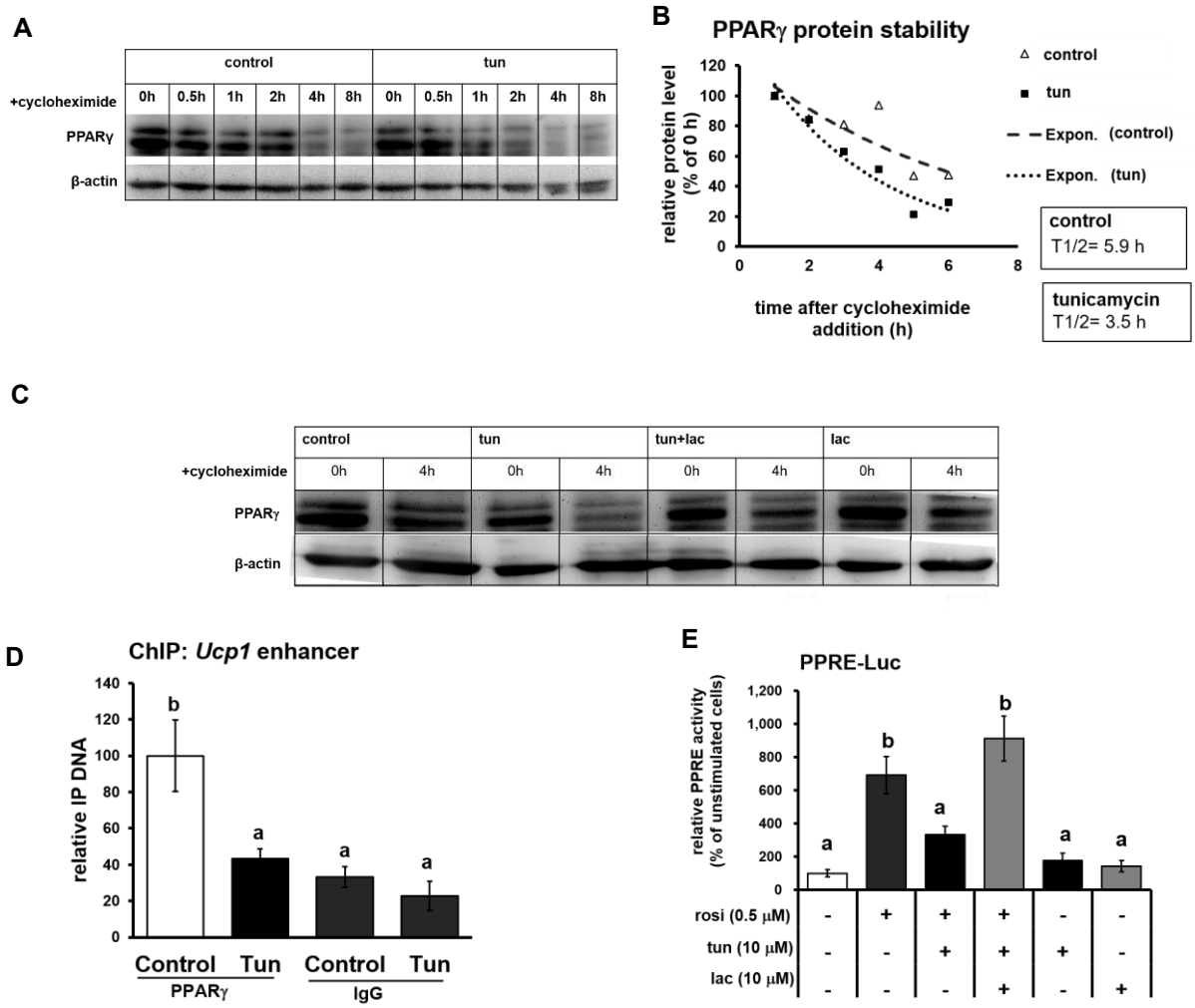

Figure 16. ER stress induces PPARγ degradation and reduces its binding activity in IWAT cells. (**A**) PPARγ protein level in cells during the cycloheximide chase experiment (20 μg/mL) at different time points with or without 1 μM tun treatment. (**B**) Regression analysis of PPARγ protein stability of (**A**). (**C**) PPARγ protein level after treated with 1 μM tun and/or 10 μM proteasome inhibitor, lactacystin (lac) for 4 h in the presence of cycloheximide (20 μg/mL). β-actin was used as a loading control. (**D**) PPAR response element (PPRE) transcriptional activity in undifferentiated IWAT cells after treated with 0.5 μM rosiglitazone (rosi) for 24 h, 10 μM tun and/or 10 μM lac for 4 h, based on a luciferase assay. (**E**) PPARγ recruitment level in the *Ucp1* distal enhancer region analyzed by chromatin immunoprecipitation (ChIP) assay after cells were treated with 1 μM tun. IgG was used as a mock control. Data are presented as mean ± S.E.M. (error bars). n = 3–5 in each group. Different letters indicate significant differences ($p < 0.05$) according to one-way ANOVA followed by Tukey–Kramer multiple.

To further examine the consequence of PPARγ degradation for its role as activator, luciferase assay was done to analyze PPAR response element (PPRE) transcriptional activity under tunicamycin stimulation. Although it was in undifferentiated IWAT cells, a luciferase assay clearly showed that the tunicamycin treatment canceled the upregulation of PPRE transcriptional activity by rosiglitazone (Figure 16D). However, the stabilization of PPARγ by lactacystin altered PPRE activity (Figure 16D), indicating that PPARγ degradation indeed affects its binding activity. To finally connect the decrease in PPARγ binding activity to *Ucp1* expression, we performed ChIP assay to measure the recruitment of PPARγ onto the PPRE within the *Ucp1* enhancer region. As shown in Figure 16E, the recruitment level of PPARγ to *Ucp1* promoter was significantly decreased after tunicamycin treatment. These data established that ER stress-induced PPARγ degradation was associated with the downregulated *Ucp1* expression due to the loss of PPARγ activator binding to *Ucp1* promoter.

ER stress suppressed both *Ucp1* mRNA and protein expression in adipose tissue

After observing a negative regulation of ER stress on *Ucp1* expression in vitro, we next investigated if the same phenomena also occur in vivo. Browning of WAT was induced by injecting PPARγ agonist (rosiglitazone) for 10 days. As shown by the expression level of ER stress marker genes *Bip* and *Chop* (Figure 17A), the rosiglitazone treatment had no effect on ER stress. IWAT, known as the most typical browning-stimulated WAT, was confirmed to undergo browning through a significant increase in *Ucp1* mRNA level (Figure 17A) after rosiglitazone treatment. After beige adipocytes were developed in IWAT, ER stress was afflicted through tunicamycin treatment. A single injection of tunicamycin could stimulate ER stress in IWAT as indicated by elevated *Bip* and *Chop* (Figure 17A) mRNA level. In this state, tunicamycin canceled *Ucp1* mRNA upregulation by rosiglitazone to basal level (Figure 17A). However, similar to in vitro result, ERK and JNK inhibition could ameliorate the tunicamycin-suppressed *Ucp1*

expression ex vivo (Figure 17B). It is important to note that ERK and JNK inhibition barely altered ER stress marker (*Bip*, *Chop*, and *Xbp1s*) (Figure 17B), suggesting that the alteration of ERK and JNK pathway possibly only affect the downstream signaling of UPR, which in this case was *Ucp1* regulation.

As mRNA expression was reduced, the UCP1 protein level was subsequently decreased under ER stress stimulation (Figure 17C). The UCP1 downregulation was also observed via immunohistochemistry (IHC) of UCP1 (Figure 17D) in IWAT. Hematoxylin and eosin (H&E) staining showed an increasing size of lipid droplet after tunicamycin injection (Figure 17D), indicating a reversal of browning (whitening). These data demonstrated that ER stress is a strong negative regulator of UCP1 expression in IWAT. Following the in vitro result, we also found a significant reduction in PPARγ protein level in vivo (Figure 18), but not mRNA level (Figure 17A), suggesting the decreased PPARγ protein as the main factor for *Ucp1* downregulation during ER stress stimulation.

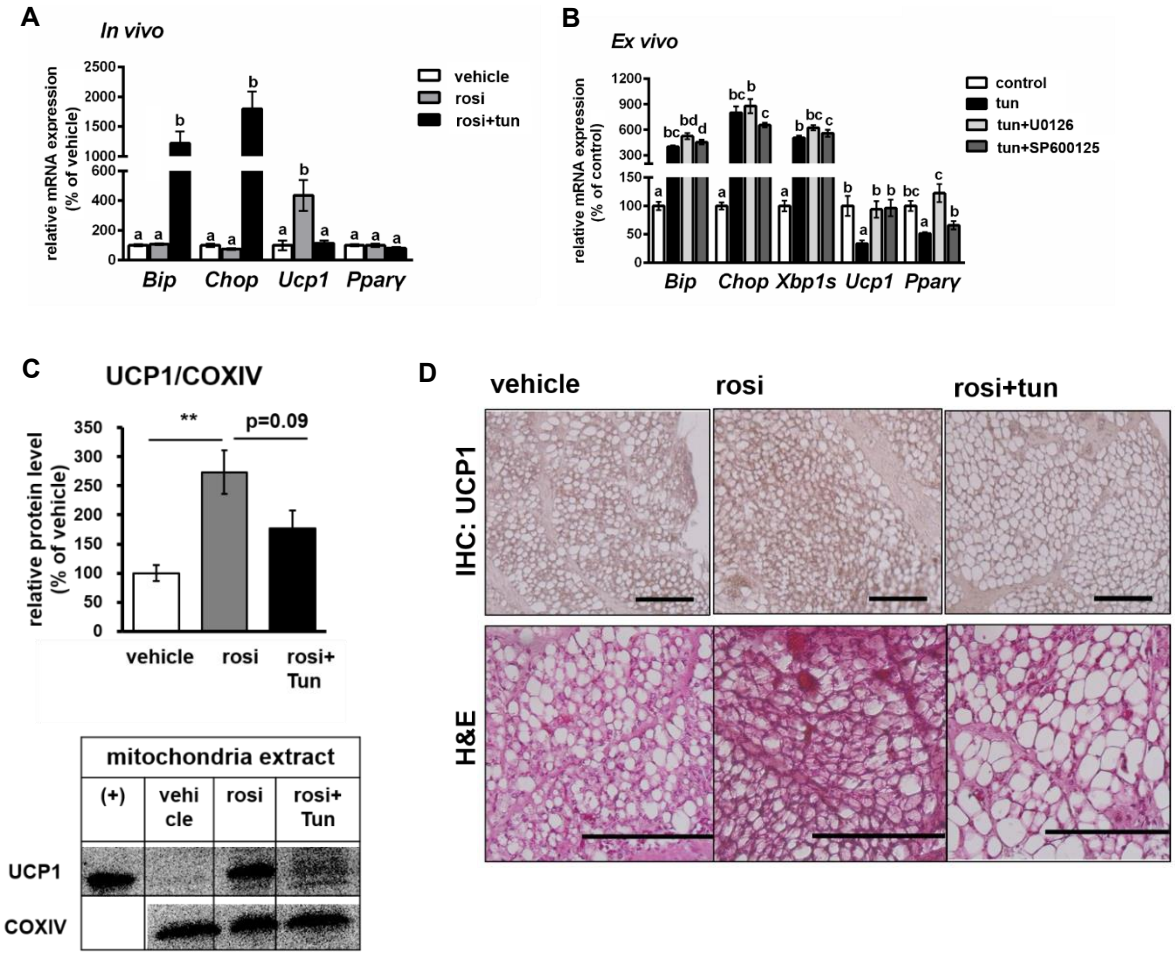

Figure 17. ER stress stimulation negatively regulates *Ucp1* expression in IWAT in vivo and ex vivo.
(**A**) The mRNA expression level of ER stress markers *Bip*, *Chop*, and *Xbp1s*, and adipocytes browning markers *Ucp1* and *Pparγ* in (A) IWAT in vivo of mice injected with vehicle, 10 mg/kg rosi for 10 days (rosi), or rosi and 10 mg/kg tun (rosi+tun) for the last 24 h or (**B**) IWAT ex vivo after treated with 1 μM tun for 24 h with or without 100 μM U0126 for 26 h and 25 μM SP600125 for 25 h. (**C**) UCP1 protein level, and (**D**) immunohistochemistry (IHC) of UCP1 (scale bar 200 μM) as well as hematoxylin and eosin (H&E) staining (scale bar 500 μM) in IWAT in vivo. (+) indicates the positive control (brown adipose tissue). Cytochrome c oxidase subunit IV (COXIV) were used as loading controls. Data are presented as mean ± S.E.M. (error bars). n = 3–8 in each group. Different letters indicate significant differences ($p < 0.05$) according to one-way ANOVA followed by Tukey–Kramer multiple comparison test. ** indicates significant differences ($p < 0.01$) according to unpaired-t test. N.S., not significant.

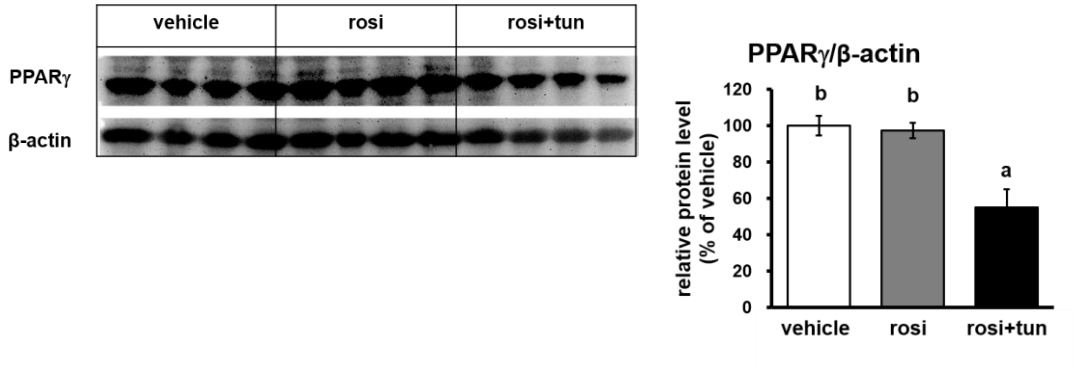

Figure 18. ER stress reduced PPARγ protein in IWAT.

PPARγ protein level in IWAT of mice injected with vehicle, 10 mg/kg rosi for 10 days, or rosi and 10 mg/kg tuni (rosi+tun) for the last 24 h. β-actin were used as loading controls. Data are presented as mean ± S.E.M. (error bars). n = 3–8 in each group. Different letters indicate significant differences ($p < 0.05$) according to one-way ANOVA followed by Tukey–Kramer multiple comparison test.

3. Discussion

ER stress and inflammation have been known as a hallmark of metabolic syndrome. While how inflammation could defect *Ucp1* expression in adipose tissue has been reported [83,92], the effect of ER stress in UCP1 regulation is still unclear. However, as shown in Figure 17C, UCP1 protein level was not detected in the basal level of IWAT (without rosiglitazone). Subsequently, UCP1 protein level remained undetected when ER stress was induced by tunicamycin (data not shown). Therefore, we decided to investigate the effect of ER stress specifically in beige adipocytes. We first needed to induce the formation of beige adipocytes in IWAT by using drug-induced BAT activation. Among those, β3-adrenergic receptor agonist (such as isoproterenol) and the activators of PPARγ (such as rosiglitazone) have been widely used for treating obesity and type 2 diabetes through the browning-related modification in carbohydrate and lipid metabolism [14,93]. Isoproterenol and rosiglitazone themselves have been reported to increase the level of *Ucp1* mRNA in adipocytes, thus both drugs can be used to induce beige adipocytes [14,94–96]. However, isoproterenol is reported to stimulate ER stress [97] while activating *Ucp1*, as confirmed in our preliminary experiment (data not shown), therefore using isoproterenol did not fit this study. Unlike isoproterenol, rosiglitazone could induce browning in beige adipocytes

without afflicting ER stress, which is shown in this report. Hence, the use of rosiglitazone would not hinder the main ER stress stimulator from tunicamycin. It is also important to note that the long treatment of rosiglitazone has been reported to have adverse effects such as weight gain (due to fluid retention) and the expansion of adipose tissue in many studies [98]. However, we have confirmed that our experimental model was done with no side effect in body weight (data not shown) or adipose tissue expansion (Figure 17D).

PPARγ has been widely known as an important activator that could influence *Ucp1* expression [8,21,55]. Interestingly, we found that PPARγ protein level is decreased under ER stress stimulation even at the basal level (data not shown). Thus, there is a possibility that ER stress-reduced PPARγ protein would further affect *Ucp1* expression and prevent WAT to undergo browning. Although this possibility could not be proven due to low UCP1 detection in WAT, our study clearly shows that ER stress was indeed a strong negative regulator of both *Ucp1* mRNA and protein expression in beige adipocytes. Furthermore, ER stress stimulation seemed to increase the lipid droplet size even in the activated beige adipocytes, which indicates whitening (reversal of browning) as shown in this study, suggesting ER stress may closely involve to the impaired browning. To find the mechanism under ER stress-suppressed *Ucp1* expression, we first noticed the major involvement of MAPK pathways: ERK and JNK as a part of UPR during ER stress. Among the three ER stress sensors that have been established, IRE1 activation has been reported to promote the phosphorylation of ERK and JNK [74,81,99], which was also shown in this study. However, the consequences of ERK and JNK activation to *Ucp1* expression during ER stress is unknown. Herein, we found that both ERK and JNK inhibition could recover *Ucp1* expression under ER stress condition, suggesting that ER stress suppressed-*Ucp1* expression might be mediated through ERK and JNK pathways. Furthermore, *Pparγ* regulation by ERK and JNK during ER stress stimulation seemed to have similar pattern as *Ucp1*. Following that, PPARγ protein level was also decreased by tunicamycin treatment. However, only JNK inhibition could

rescue PPARγ protein level. These results suggesting that the reduced *Ucp1* expression was mediated preferably through JNK-PPARγ interaction.

It has been known that PPARγ is a phosphorylation target of MAPK which includes ERK and JNK [91]. PPARγ phosphorylation at Serine 112 by either ERK or JNK has been known to change PPARγ conformation that lead to the protein degradation and repressed transcriptional activation [91,100]. However, to our surprise, we did not find significant change in phosphorylation of PPARγ. Instead, PPARγ protein level was decreased earlier than its phosphorylation. Thus, we assume that although JNK-mediated the reduction of PPARγ activity by phosphorylation has been established through several studies [91,100,101], the detail mechanism may be different depending on the source of JNK activation. In the case of ER stress, JNK might mediate the decrease of *Pparγ* mRNA and protein level independent of phosphorylation modification. Accordingly, JNK activation is also known to be associated with apoptosis through promoting phosphorylation and activation of pro-apoptotic protein Bcl-2-associated X protein (Bax) [74,102,103]. Indeed, we found that chronic ER stress (12–20 h) in our experimental condition induced cell apoptosis, indicated by the upregulated *Chop* expression, decreased cell viability, and increased in cleavage Caspase3. *Chop* has been reported to participate in cell death program during ER stress [104]. On the other hand, Caspase3 (apoptosis marker) has been found to mediate PPARγ cleavage [105]. These pieces of evidence suggest that JNK-mediated reduced PPARγ activity may be related to the cell apoptosis response.

Regardless, we found a consistent decrease in PPARγ activity in vitro, ex vivo, and in vivo after ER stress stimulation. Indeed, when we reduced PPARγ activity by PPARγ antagonist (GW9662), it similarly downregulated *Ucp1* expression as tunicamycin. Furthermore, the co-treatment between tunicamycin and GW9662 did not enhance the suppression of *Ucp1* expression, suggesting that both compounds regulated *Ucp1* expression preferably through the same pathway, which in this case was through PPARγ. To finally connect the consequence of PPARγ reduction

to *Ucp1* expression, we investigated the PPRE activity under tunicamycin treatment. *Ucp1* is one of the established activation target of PPARγ in adipose tissue, equipped with PPRE binding sequence located on the *Ucp1* distal enhancer (-2494 to -2318 bp) [8]. Herein, we showed that PPRE activity was significantly affected after ER stress stimulation, based on the luciferase assay. Although it was performed in undifferentiated IWAT cells due to the low transfection efficiency in differentiated cells, we further confirmed in ChIP assay that PPARγ recruitment to *Ucp1* promoter was consistently reduced in differentiated IWAT cells.

These pieces of evidence thus show that the reduced PPARγ binding to *Ucp1* promoter are likely due to the decreased protein level and subsequently affected *Ucp1* mRNA downregulation as ER stress was stimulated. While the reduced *Pparγ* mRNA expression was only seen in vitro, the PPARγ protein level was decreased both in vitro and in vivo. These results might indicate that the loss of PPARγ protein was not dependent on its mRNA expression. Later, we found that PPARγ protein stability was disturbed by ER stress stimulation, suggesting that PPARγ protein was degraded. In addition, it has been known that ER stress induction could lead to the activation of protein degradation pathway to remove the accumulation of unfolded protein [75]. Basically, there are two major protein degradation pathways: proteasomes (via ER-associated degradation or ERAD) and lysosome (via autophagy) degradation [75,106]. Between two pathways, ERAD is recognized as the predominant cellular mechanism for removal of unfolded protein [75,107]. Certainly, the addition of proteasome inhibitor (lactacystin) rescued PPARγ protein and PPRE activity, suggesting proteasome-mediated PPARγ degradation affects its binding activity to *Ucp1* promoter during ER stress stimulation in beige adipocytes. Interestingly, the induction of ER stress did not only affect *Ucp1* mRNA expression, but also UCP1 protein level. Although, it might be linear to the decreased in mRNA expression, there still has possibility that the reduced UCP1 protein level was affected directly through ERAD mechanism. Therefore, further investigation is needed to carefully assess UCP1 protein modification in ER stress. Regardless, the present study

highlights a novel mechanism of ER stress regulation to *Ucp1* expression preferentially via the suppression of activator PPARγ in beige adipocytes. Furthermore, it may provide a solid foundation about the involvement of ER stress to the impaired thermogenic capacity, especially in obese adipose tissue. Thus, recovering ER stress is proven essential to rescue thermogenic activity in adipose tissue.

Summary

Chapter 1

The induction of beige adipocytes has been expected as a potential way to treat obesity, marked by the upregulation of *Ucp1*. Improving *Ucp1* expression increases the thermogenesis capacity and further affects the whole-body metabolism. On the other hand, histone modification has emerged as a new approach of study to regulate gene expression through chromatin structure remodeling. Indeed, this study found that there is an additional novel pathway within β-AR stimulated-*Ucp1* expression, which is regulated by the change of chromatin state specifically in the *Ucp1* promoter in beige adipocytes. Further, this mechanism was specifically mediated through HDAC3 inhibition. β-AR stimulation simultaneously downregulated the mRNA and protein level of HDAC3, a chromatin modifier, which accompanied the increased acetylation in the histone activation mark H3K27ac within *Ucp1* promoter, indicating a favorable open chromatin structure for gene expression. The important role of HDAC3 in β-AR stimulation was further proved through the enhanced *Ucp1* expression when HDAC3 was specifically inhibited. Hence, our study proposing HDAC3 inhibition as a new potential target to enhance *Ucp1* expression in beige adipocytes.

Chapter 2

Besides epigenetic mechanism, *Ucp1* expression could also be regulated through physiological conditions such as obesity. Indeed, UCP1 expression was impaired in obese adipose tissue. Although obesity is characterized by various metabolic symptoms such as ER stress and others, the specific factor that could regulate the impairment of *Ucp1* expression is still unclear. ER stress itself has been known as a hallmark of obese adipose tissue marked through the enhancement of ER stress marker during obesity. Indeed, our study found that ER stress greatly contributes to the impaired *Ucp1* expression in beige adipocytes. Further investigations showed

that ERK and JNK were both activated and they regulated not only *Ucp1*, but also *Pparγ* mRNA expression. Following this change in mRNA level, PPARγ protein was also severely degraded under ER stress stimulation. PPARγ has been known as an important activator that could regulate *Ucp1* expression. Indeed, PPRE-mediated transcriptional activity and PPARγ protein recruitment to *Ucp1* promoter were significantly decreased, as a consequence of protein degradation. Additionally, only JNK inhibition, but not ERK, rescued the PPARγ protein reduction, suggesting ER stress-induced PPARγ degradation preferably mediated through JNK pathway. These findings showed a novel mechanism of ER stress-suppressed *Ucp1* expression is mediated through JNK-induced PPARγ protein reduction. Thus, inhibiting ER stress is necessary to prevent the impairment of *Ucp1* expression in beige adipocytes.

In conclusion, our study showed novel pathways of adipocytes browning marker–*Ucp1* regulation in beige adipocytes through epigenetic modification and ER stress. We found that β-AR stimulation-induced *Ucp1* expression was also mediated through the suppression of HDAC3 activity. On top of that, ER stress, which is a hallmark of obesity, greatly downregulated *Ucp1* expression. Based on these findings, we suggests a chromatin modifier (specifically through HDAC3 inhibition) and ER stress inhibitor as potential characteristics to improve browning of WAT.

Acknowledgements

The author would like to give the greatest appreciation to Dr. Teruo Kawada, Professor of Graduate School of Agriculture, Kyoto University for giving a chance to have a wonderful experience to study in his laboratory. His endless support and excellent guidance have contributed greatly to the completion of this study.

The author is also sincerely thankful to Dr. Tsuyoshi Goto, Associate Professor of Graduate School of Agriculture, Kyoto University and Dr. Huei-Fen Jheng, Assistant Professor of Graduate School of Agriculture, Kyoto University, for giving their valuable time in discussion and diligently monitoring the research progress.

The author also wants to extend gratefulness to Dr. Wataru Nomura, Assistant Professor of Graduate School of Agriculture, Kyoto University, Dr. Takeshi Ara, Associate Professor of Graduate School of Agriculture, Kyoto University, and Dr. Haruya Takahashi, Assistant Professor of Graduate School of Agriculture, Kyoto University for their sincere encouragement and valuable advices they have always provided during the study.

In addition, the author would like to gratefully thank Dr. Kazuhiro Irie, Professor of Graduate School of Agriculture, Kyoto University and Dr. Kazuo Inoue, Professor of Graduate School of Agriculture, Kyoto University for their valued advice and support on the completion of the study.

The author also enthusiastically thank you Ms. Sayoko Shinoto and Ms. Rika Yoshii for their secretarial support, and Mr. Masaomi Komori for his technical support.

Further warm appreciation was sent preciously to Indonesia Endowment Fund (LPDP), Ministry of Finance, Indonesia, for generously funding my study. I love Indonesia and will come back to contribute to my country.

The author would like to give special gratitude to the fellow members in the Laboratory of Molecular Function of Food, Graduate School of Agriculture, Kyoto University for their kind encouragement and friendly atmosphere throughout the study.

Finally, the author profoundly thanks the beloved family and friends in Indonesia for their prayers and constant support in my life.

The present work was done in the Laboratory of Molecular Function of Food, Division of Food Science and Biotechnology, Graduate School of Agriculture, Kyoto University.

Ana Yuliana

References

1. Kwok, K. H. M.; Lam, K. S. L.; Xu, A. Heterogeneity of white adipose tissue: Molecular basis and clinical implications. *Experimental and Molecular Medicine* **2016**, *48*, e215-12, doi:10.1038/emm.2016.5.
2. Smorlesi, A.; Frontini, A.; Giordano, A.; Cinti, S. The adipose organ: White-brown adipocyte plasticity and metabolic inflammation. *Obesity Reviews* **2012**, *13*, 83–96, doi:10.1111/j.1467-789X.2012.01039.x.
3. Bartelt, A.; Heeren, J. Adipose tissue browning and metabolic health. *Nature Publishing Group* **2013**, *10*, 24–36, doi:10.1038/nrendo.2013.204.
4. Cannon, B.; Nedergaard, J. Brown adipose tissue: function and physiological significance. *Physiological reviews* **2004**, *84*, 277–359.
5. Gómez-Hernández, A.; Beneit, N.; Díaz-Castroverde, S.; Escribano, Ó. Differential Role of Adipose Tissues in Obesity and Related Metabolic and Vascular Complications. *International Journal of Endocrinology* **2016**, *2016*, 1–15, doi:10.1155/2016/1216783.
6. Pellegrinelli, V.; Carobbio, S.; Vidal-Puig, A. Adipose tissue plasticity: how fat depots respond differently to pathophysiological cues. *Diabetologia* **2016**, *59*, 1075–1088, doi:10.1007/s00125-016-3933-4.
7. Harms, M.; Seale, P. Brown and beige fat: development, function and therapeutic potential. *Nature Medicine* **2013**, *19*, 1252–1263, doi:10.1038/nm.3361.
8. Villarroya, F.; Iglesias, R.; Giralt, M. PPARs in the control of uncoupling proteins gene expression. *PPAR Research* **2007**, *2007*, doi:10.1155/2007/74364.
9. Ohyama, K.; Nogusa, Y.; Shinoda, K.; Suzuki, K.; Bannai, M.; Kajimura, S. A synergistic antiobesity effect by a combination of capsinoids and cold temperature through promoting

beige adipocyte biogenesis. *Diabetes* **2016**, *65*, 1410–1423, doi:10.2337/db15-0662.

10. Peng, X. R.; Gennemark, P.; O'Mahony, G.; Bartesaghi, S. Unlock the thermogenic potential of adipose tissue: Pharmacological modulation and implications for treatment of diabetes and obesity. *Frontiers in Endocrinology* **2015**, *6*, doi:10.3389/fendo.2015.00174.
11. Xue, B.; Coulter, A.; Rim, J. S.; Koza, R. a; Kozak, L. P. Transcriptional Synergy and the Regulation of Ucp1 during Brown Adipcytes Induction in White Fat Depots. *Molecular and cellular biology* **2005**, *25*, 8311–8322, doi:10.1128/MCB.25.18.8311.
12. S Collins, E Yehuda-Shnaidman, H. W. Positive and negative control of Ucp1 gene transcription and the role of b-adrenergic signaling networks. *International Journal of Obesity* **2010**, *34*, S28–S33, doi:10.1038/ijo.2010.180.
13. Kalinovich, A. V.; de Jong, J. M. A.; Cannon, B.; Nedergaard, J. UCP1 in adipose tissues: two steps to full browning. *Biochimie* **2017**, *134*, 127–137, doi:10.1016/j.biochi.2017.01.007.
14. Mukherjee, J.; Baranwal, A.; N. Schade, K. Classification of Therapeutic and Experimental Drugs for Brown Adipose Tissue Activation: Potential Treatment Strategies for Diabetes and Obesity. *Current Diabetes Reviews* **2016**, *12*, 414–428, doi:10.2174/1573399812666160517115450.
15. Martínez, J. A.; Milagro, F. I.; Claycombe, K. J.; Schalinske, K. L. Epigenetics in Adipose Tissue , Obesity , Weight Loss , and Diabetes 1 , 2. *Advances in Nutrition* **2014**, *5*, 71–81, doi:10.3945/an.113.004705.71.
16. Simmons, D. Epigenetic Influences and Disease. *Nature Education 1* **2008**, *1*, 6.
17. Ling, C.; Groop, L. Epigenetics: A molecular link between environmental factors and type 2 diabetes. *Diabetes* **2009**, *58*, 2718–2725, doi:10.2337/db09-1003.
18. Pagliassotti, M. J.; Kim, P. Y.; Estrada, A. L.; Stewart, C. M.; Gentile, C. L. Endoplasmic

reticulum stress in obesity and obesity-related disorders: An expanded view. *Metabolism: Clinical and Experimental* **2016**, *65*, 1238–1246, doi:10.1016/j.metabol.2016.05.002.

19. Alcalá, M.; Calderon-Dominguez, M.; Bustos, E.; Ramos, P.; Casals, N.; Serra, D.; Viana, M.; Herrero, L. Increased inflammation, oxidative stress and mitochondrial respiration in brown adipose tissue from obese mice. *Scientific Reports* **2017**, *7*, 1–12, doi:10.1038/s41598-017-16463-6.

20. Hetz, C.; Chevet, E.; Harding, H. P. Targeting the unfolded protein response in disease. *Nature Reviews Drug Discovery* **2013**, *12*, 703–719, doi:10.1038/nrd3976.

21. Xue, B.; Coulter, A.; Rim, J. S.; Koza, R. A.; Kozak, L. P. Transcriptional Synergy and the Regulation of. *Molecular and cellular biology* **2005**, *25*, 8311–8322, doi:10.1128/MCB.25.18.8311.

22. Mottillo, E. P.; Balasubramanian, P.; Lee, Y.-H.; Weng, C.; Kershaw, E. E.; Granneman, J. G. Coupling of lipolysis and de novo lipogenesis in brown, beige, and white adipose tissues during chronic β3-adrenergic receptor activation. *Journal of Lipid Research* **2014**, *55*, 2276–2286, doi:10.1194/jlr.M050005.

23. Carey, A. L.; Formosa, M. F.; Van Every, B.; Bertovic, D.; Eikelis, N.; Lambert, G. W.; Kalff, V.; Duffy, S. J.; Cherk, M. H.; Kingwell, B. A. Ephedrine activates brown adipose tissue in lean but not obese humans. *Diabetologia* **2013**, *56*, 147–155, doi:10.1007/s00125-012-2748-1.

24. Redman, L. M.; de Jonge, L.; Fang, X.; Gamlin, B.; Recker, D.; Greenway, F. L.; Smith, S. R.; Ravussin, E. Lack of an Effect of a Novel β_3 -Adrenoceptor Agonist, TAK-677, on Energy Metabolism in Obese Individuals: A Double-Blind, Placebo-Controlled Randomized Study. *The Journal of Clinical Endocrinology & Metabolism* **2007**, *92*, 527–531, doi:10.1210/jc.2006-1740.

25. Shahbazian, M. D.; Grunstein, M. Functions of Site-Specific Histone Acetylation and Deacetylation. *Annual Review of Biochemistry* **2007**, *76*, 75–100, doi:10.1146/annurev.biochem.76.052705.162114.

26. Galmozzi, A.; Mitro, N.; Ferrari, A.; Gers, E.; Gilardi, F.; Godio, C.; Cermenati, G.; Gualerzi, A.; Donetti, E.; Rotili, D.; Valente, S.; Guerrini, U.; Caruso, D.; Mai, A.; Saez, E.; De Fabiani, E.; Crestani, M. Inhibition of class i histone deacetylases unveils a mitochondrial signature and enhances oxidative metabolism in skeletal muscle and adipose tissue. *Diabetes* **2013**, *62*, 732–742, doi:10.2337/db12-0548.

27. Li, F.; Wu, R.; Cui, X.; Zha, L.; Yu, L.; Shi, H.; Xue, B. Histone deacetylase 1 (HDAC1) negatively regulates thermogenic program in brown adipocytes via coordinated regulation of histone H3 lysine 27 (H3K27) deacetylation and methylation. *Journal of Biological Chemistry* **2016**, *291*, 4523–4536, doi:10.1074/jbc.M115.677930.

28. Ferrari, A.; Longo, R.; Fiorino, E.; Silva, R.; Mitro, N.; Cermenati, G.; Gilardi, F.; Desvergne, B.; Andolfo, A.; Magagnotti, C.; Caruso, D.; Fabiani, E. De; Hiebert, S. W.; Crestani, M. HDAC3 is a molecular brake of the metabolic switch supporting white adipose tissue browning. *Nature Communications* **2017**, *8*, 93, doi:10.1038/s41467-017-00182-7.

29. Heintzman, N. D.; Hon, G. C.; Hawkins, R. D.; Kheradpour, P.; Stark, A.; Harp, L. F.; Ye, Z.; Lee, L. K.; Stuart, R. K.; Ching, C. W.; Ching, K. A.; Antosiewicz-Bourget, J. E.; Liu, H.; Zhang, X.; Green, R. D.; Lobanenkov, V. V.; Stewart, R.; Thomson, J. A.; Crawford, G. E.; Kellis, M.; Ren, B. Histone modifications at human enhancers reflect global cell-type-specific gene expression. *Nature* **2009**, *459*, 108–112, doi:10.1038/nature07829.

30. Creyghton, M. P.; Cheng, A. W.; Welstead, G. G.; Kooistra, T.; Carey, B. W.; Steine, E. J.; Hanna, J.; Lodato, M. A.; Frampton, G. M.; Sharp, P. A.; Boyer, L. A.; Young, R. A.;

Jaenisch, R. Histone H3K27ac separates active from poised enhancers and predicts developmental state. *Proceedings of the National Academy of Sciences* **2010**, *107*, 21931–21936, doi:10.1073/pnas.1016071107.

31. Calo, E.; Wysocka, J. Modification of enhancer chromatin: what, how and why? *Molecular Cell* **2013**, *49*, 1–24, doi:10.1016/j.molcel.2013.01.038.

32. Roche, J.; Bertrand, P. Inside HDACs with more selective HDAC inhibitors. *European journal of medicinal chemistry* **2016**, *121*, 451–483, doi:10.1016/j.ejmech.2016.05.047.

33. de Ruijter, A. J. M.; van Gennip, A. H.; Caron, H. N.; Kemp, S.; van Kuilenburg, A. B. P. Histone deacetylases (HDACs): characterization of the classical HDAC family. *The Biochemical journal* **2003**, *370*, 737–49, doi:10.1042/BJ20021321.

34. Jia, Y.; Hong, J.; Li, H.; Hu, Y.; Jia, L.; Cai, D.; Zhao, R. Butyrate stimulates adipose lipolysis and mitochondrial OXPHOS through histone hyperacetylation-associated AR3β activation in high-fat diet-induced obese mice. *Experimental Physiology* **2016**, *2*, 273–281, doi:10.1113/EP086114.

35. Chriett, S.; Zerzaihi, O.; Vidal, H.; Pirola, L. The histone deacetylase inhibitor sodium butyrate improves insulin signalling in palmitate-induced insulin resistance in L6 rat muscle cells through epigenetically-mediated up-regulation of Irs1. *Molecular and Cellular Endocrinology* **2017**, *439*, 224–232, doi:10.1016/j.mce.2016.09.006.

36. Rumberger, J. M.; Arch, J. R. S.; Green, A. Butyrate and other short-chain fatty acids increase the rate of lipolysis in 3T3-L1 adipocytes. *PeerJ* **2014**, *2*, e611, doi:10.7717/peerj.611.

37. Ye, J. Improving insulin sensitivity with HDAC inhibitor. *Diabetes* **2013**, *62*, 685–687, doi:10.2337/db12-1354.

38. Ferrari, A.; Fiorino, E.; Longo, R.; Barilla, S.; Mitro, N.; Cermenati, G.; Giudici, M.;

Caruso, D.; Mai, A.; Guerrini, U.; De Fabiani, E.; Crestani, M. Attenuation of diet-induced obesity and induction of white fat browning with a chemical inhibitor of histone deacetylases. *International Journal Of Obesity* **2016**, *41*, 289.

39. Hirai, S.; Uemura, T.; Mizoguchi, N.; Lee, J. Y.; Taketani, K.; Nakano, Y.; Hoshino, S.; Tsuge, N.; Narukami, T.; Yu, R.; Takahashi, N.; Kawada, T. Diosgenin attenuates inflammatory changes in the interaction between adipocytes and macrophages. *Molecular Nutrition and Food Research* **2010**, *54*, 797–804, doi:10.1002/mnfr.200900208.

40. Kang, M. S.; Hirai, S.; Goto, T.; Kuroyanagi, K.; Lee, J. Y.; Uemura, T.; Ezaki, Y.; Takahashi, N.; Kawada, T. Dehydroabietic acid, a phytochemical, acts as ligand for PPARs in macrophages and adipocytes to regulate inflammation. *Biochemical and Biophysical Research Communications* **2008**, *369*, 333–338, doi:10.1016/j.bbrc.2008.02.002.

41. Yang, H. E.; Li, Y.; Nishimura, A.; Jheng, H. F.; Yuliana, A.; Kitano-Ohue, R.; Nomura, W.; Takahashi, N.; Kim, C. S.; Yu, R.; Kitamura, N.; Park, S. B.; Kishino, S.; Ogawa, J.; Kawada, T.; Goto, T. Synthesized enone fatty acids resembling metabolites from gut microbiota suppress macrophage-mediated inflammation in adipocytes. *Molecular Nutrition and Food Research* **2017**, *61*, 1–13, doi:10.1002/mnfr.201700064.

42. Chiocca, S.; Segré, C. V. Regulating the regulators: The post-translational code of class i HDAC1 and HDAC2. *Journal of Biomedicine and Biotechnology* **2011**, *2011*, doi:10.1155/2011/690848.

43. Mihaylova, M. M.; Shaw, R. J. Metabolic reprogramming by class I and II histone deacetylases. *Trends in Endocrinology and Metabolism* **2013**, *24*, 48–57, doi:10.1016/j.tem.2012.09.003.

44. Lee, H.; Rezai-Zadeh, N.; Seto, E. Negative regulation of histone deacetylase 8 activity by cyclic AMP-dependent protein kinase A. *Molecular and cellular biology* **2004**, *24*,

765–73, doi:10.1128/MCB.24.2.765.

45. Brandl, A.; Heinzel, T.; Krämer, O. H. Histone deacetylases: salesmen and customers in the post-translational modification market. *Biology of the Cell* **2009**, *101*, 193–205, doi:10.1042/BC20080158.

46. Henagan, T. M.; Stefanska, B.; Fang, Z.; Navard, A. M.; Ye, J.; Lenard, N. R.; Devarshi, P. P. Sodium butyrate epigenetically modulates high-fat diet-induced skeletal muscle mitochondrial adaptation, obesity and insulin resistance through nucleosome positioning. *British Journal of Pharmacology* **2015**, *172*, 2782–2798, doi:10.1111/bph.13058.

47. Hong, J.; Jia, Y.; Pan, S.; Jia, L.; Li, H.; Han, Z.; Cai, D.; Zhao, R. Butyrate alleviates high fat diet-induced obesity through activation of adiponectin-mediated pathway and stimulation of mitochondrial function in the skeletal muscle of mice. *Oncotarget* **2016**, *7*, 56071–56082, doi:10.18632/oncotarget.11267.

48. Leus, N. G. J.; Van Der Wouden, P. E.; Van Den Bosch, T.; Hooghiemstra, W. T. R.; Ourailidou, M. E.; Kistemaker, L. E. M.; Bischoff, R.; Gosens, R.; Haisma, H. J.; Dekker, F. J. HDAC 3-selective inhibitor RGFP966 demonstrates anti-inflammatory properties in RAW 264.7 macrophages and mouse precision-cut lung slices by attenuating NF-κB p65 transcriptional activity. *Biochemical Pharmacology* **2016**, *108*, 58–74, doi:10.1016/j.bcp.2016.03.010.

49. Cardinale, J. P.; Sriramula, S.; Pariaut, R.; Guggilam, A.; Mariappan, N.; Elks, C. M.; Francis, J. HDAC Inhibition Attenuates Inflammatory, Hypertrophic, and Hypertensive Responses in Spontaneously Hypertensive Rats. *Hypertension* **2010**, *56*, 437–444, doi:10.1161/HYPERTENSIONAHA.110.154567.

50. Qiu, X.; Xiao, X.; Li, N.; Li, Y. Histone deacetylases inhibitors (HDACis) as novel therapeutic application in various clinical diseases. *Progress in Neuro-*

Psychopharmacology and Biological Psychiatry **2017**, *72*, 60–72, doi:10.1016/j.pnpbp.2016.09.002.

51. Lin, J.; Handschin, C.; Spiegelman, B. M. Metabolic control through the PGC-1 family of transcription coactivators. *Cell Metabolism* **2005**, *1*, 361–370, doi:10.1016/j.cmet.2005.05.004.

52. Delcuve, G. P.; Khan, D. H.; Davie, J. R. Roles of histone deacetylases in epigenetic regulation: emerging paradigms from studies with inhibitors. *Clinical epigenetics* **2012**, *4*, 5, doi:10.1186/1868-7083-4-5.

53. Emmett, M. J.; Lim, H.; Jager, J.; Richter, H. J.; Adlanmerini, M.; Peed, L. C.; Briggs, E. R.; Steger, D. J.; Ma, T.; Sims, C. A.; Baur, J. A.; Pei, L.; Won, K.; Seale, P.; Gerhart-Hines, Z.; Lazar, M. A. Histone deacetylase 3 prepares brown adipose tissue for acute thermogenic challenge. *Nature* **2017**, *546*, 544–548, doi:10.1038/nature22819.

54. Cao, W.; Medvedev, A. V.; Daniel, K. W.; Collins, S. beta-adrenergic activation of p38 MAP kinase in adipocytes: cAMP induction of the uncoupling protein 1 (UCP1) gene requires p38 map kinase. *Journal of Biological Chemistry* **2001**, *276*, 27077–27082, doi:10.1074/jbc.M101049200.

55. Chen, H. Y.; Liu, Q.; Salter, A. M.; Lomax, M. A. Synergism between cAMP and PPARγ Signalling in the Initiation of UCP1 Gene Expression in HIB1B Brown Adipocytes. *PPAR Research* **2013**, *2013*, 1–8, doi:10.1155/2013/476049.

56. Choudhary, C.; Kumar, C.; Gnad, F.; Nielsen, M. L.; Rehman, M.; Walther, T. C.; Olsen, J. V; Mann, M. Lysine acetylation targets protein complexes and co-regulated major cellular functions. *Science* **2009**, *325*, 834–840, doi:10.1126/science.1175371.

57. Wolfson, N. A.; Ann Pitcairn, C.; Fierke, C. A. HDAC8 substrates: Histones and beyond. *Biopolymers* **2013**, *99*, 112–126, doi:10.1002/bip.22135.

58. Yang, W. M.; Yao, Y. L. Beyond histone and deacetylase: An overview of cytoplasmic histone deacetylases and their nonhistone substrates. *Journal of Biomedicine and Biotechnology* **2011**, *2011*, doi:10.1155/2011/146493.

59. Chakrabarti, A.; Oehme, I.; Witt, O.; Oliveira, G.; Sippl, W.; Romier, C.; Pierce, R. J.; Jung, M. HDAC8: A multifaceted target for therapeutic interventions. *Trends in Pharmacological Sciences* **2015**, *36*, 481–492, doi:10.1016/j.tips.2015.04.013.

60. Mottamal, M.; Zheng, S.; Huang, T.; Wang, G. Histone Deacetylase Inhibitors in Clinical Studies as Templates for New Anticancer Agents. *Molecules* **2015**, *20*, 3898–3941, doi:10.3390/molecules20033898.

61. Chakrabarti, A.; Melesina, J.; Kolbinger, F. R.; Oehme, I.; Senger, J.; Witt, O.; Sippl, W.; Jung, M. Targeting histone deacetylase 8 as a therapeutic approach to cancer and neurodegenerative diseases. *Future Medicinal Chemistry* **2016**, *8*, 1609–1634.

62. Sharma, M.; Shivarama Shetty, M.; Arumugam, T. V.; Sajikumar, S. Histone deacetylase 3 inhibition re-establishes synaptic tagging and capture in aging through the activation of nuclear factor kappa B. *Scientific reports* **2015**, *5*, 16616, doi:10.1038/srep16616.

63. Christensen, D. P.; Dahllof, M.; Lundh, M.; Rasmussen, D. N.; Nielsen, M. D.; Billestrup, N.; Grunnet, L. G.; Poulsen, T. M. Histone Deacetylase (HDAC) Inhibition as a Novel Treatment as Novel Treatment for Ddiabetes Mellitus. *Molecular Medicine* **2011**, *17*, 1, doi:10.2119/molmed.2011.00021.

64. Leus, N. G. J.; Zwinderman, M. R. H.; Dekker, F. J. Histone deacetylase 3 (HDAC 3) as emerging drug target in NF-κB-mediated inflammation. *Current Opinion in Chemical Biology* **2016**, *33*, 160–168, doi:10.1016/j.cbpa.2016.06.019.

65. Arguelles, A. O.; Meruvu, S.; Bowman, J. D. Are epigenetic drugs for diabetes and obesity at our door step ? *Drug Discovery Today* **2016**, *21*, 499–509,

doi:10.1016/j.drudis.2015.12.001.

66. Sathishkumar, C.; Prabu, P.; Balakumar, M.; Lenin, R.; Prabhu, D.; Anjana, R. M.; Mohan, V.; Balasubramanyam, M. Augmentation of histone deacetylase 3 (HDAC3) epigenetic signature at the interface of proinflammation and insulin resistance in patients with type 2 diabetes. *Clinical epigenetics* **2016**, *8*, 125, doi:10.1186/s13148-016-0293-3.

67. Vitali, A.; Murano, I.; Zingaretti, M. C.; Frontini, A.; Ricquier, D.; Cinti, S. The adipose organ of obesity-prone C57BL/6J mice is composed of mixed white and brown adipocytes. *Journal of Lipid Research* **2012**, *53*, 619–629, doi:10.1194/jlr.M018846.

68. Okla, M.; Wang, W.; Kang, I.; Pashaj, A.; Carr, T.; Chung, S. Activation of Toll-like receptor 4 (TLR4) attenuates adaptive thermogenesis via endoplasmic reticulum stress. *Journal of Biological Chemistry* **2015**, *290*, 26476–26490, doi:10.1074/jbc.M115.677724.

69. Lee, Y. K.; Cowan, C. A. White to brite adipocyte transition and back again. *Nature Cell Biology* **2013**, *15*, 568–569, doi:10.1038/ncb2776.

70. Rosenwald, M.; Perdikari, A.; Rülicke, T.; Wolfrum, C. Bi-directional interconversion of brite and white adipocytes. *Nature Cell Biology* **2013**, *15*, 659–667, doi:10.1038/ncb2740.

71. Ozcan, U.; Cao, Q.; Yilmaz, E.; Lee, A.-H.; Iwakoshi, N. N.; Ozdelen, E.; Tuncman, G.; Gorgun, C.; Glimcher, L. H.; Hostamisligil, G. S. Endoplasmic Reticulum Stress Links Obesity, Insulin Action, and Type 2 Diabetes. *Science* **2003**, *299*, 1033–1036, doi:10.1126/science.1103160.

72. Lindholm, D.; Korhonen, L.; Eriksson, O.; Kõks, S. Recent Insights into the Role of Unfolded Protein Response in ER Stress in Health and Disease. *Frontiers in Cell and Developmental Biology* **2017**, *5*, 1–16, doi:10.3389/fcell.2017.00048.

73. Walter, P.; Ron, D. The Unfolded Protein Response: From Stress Pathway to Homeostatic Regulation. *Science* **2011**, *334*, 1081–1085, doi:10.1126/science.1209038.

74. Darling, N. J.; Cook, S. J. The role of MAPK signalling pathways in the response to endoplasmic reticulum stress. *Biochimica et Biophysica Acta - Molecular Cell Research* **2014**, *1843*, 2150–2163, doi:10.1016/j.bbamcr.2014.01.009.

75. Sano, R.; Reed, J. C. ER stress-induced cell death mechanisms. *Biochimica et Biophysica Acta - Molecular Cell Research* **2013**, *1833*, 3460–3470, doi:10.1016/j.bbamcr.2013.06.028.

76. Tabas, I.; Ron, D. Integrating the mechanisms of apoptosis induced by endoplasmic reticulum stress. *Nature Cell Biology* **2011**, *13*, 184–190, doi:10.1038/ncb0311-184.

77. Kawasaki, N.; Asada, R.; Saito, A.; Kanemoto, S.; Imaizumi, K. Obesity-induced endoplasmic reticulum stress causes chronic inflammation in adipose tissue. *Scientific Reports* **2012**, *2*, 1–7, doi:10.1038/srep00799.

78. Gregor, M. F.; Hotamisligil, G. S. *Thematic review series: Adipocyte Biology.* Adipocyte stress: the endoplasmic reticulum and metabolic disease. *Journal of Lipid Research* **2007**, *48*, 1905–1914, doi:10.1194/jlr.R700007-JLR200.

79. Han, J.; Kaufman, R. J. The role of ER stress in lipid metabolism and lipotoxicity. *Journal of Lipid Research* **2016**, *57*, 1329–1338, doi:10.1194/jlr.R067595.

80. Bartelt, A.; Widenmaier, S. B.; Schlein, C.; Johann, K.; Goncalves, R. L. S.; Eguchi, K.; Fischer, A. W.; Parlakgül, G.; Snyder, N. A.; Nguyen, T. B.; Bruns, O. T.; Franke, D.; Bawendi, M. G.; Lynes, M. D.; Leiria, L. O.; Tseng, Y. H.; Inouye, K. E.; Arruda, A. P.; Hotamisligil, G. S. Brown adipose tissue thermogenic adaptation requires Nrf1-mediated proteasomal activity. *Nature Medicine* **2018**, *24*, 292–303, doi:10.1038/nm.4481.

81. Salvadó, L.; Palomer, X.; Barroso, E.; Vázquez-Carrera, M. Targeting endoplasmic reticulum stress in insulin resistance. *Trends in Endocrinology and Metabolism* **2015**, *26*, 438–448, doi:10.1016/j.tem.2015.05.007.

82. Deng, J.; Liu, S.; Zou, L.; Xu, C.; Geng, B.; Xu, G. Lipolysis response to endoplasmic reticulum stress in adipose cells. *Journal of Biological Chemistry* **2012**, *287*, 6240–6249, doi:10.1074/jbc.M111.299115.

83. Sakamoto, T.; Nitta, T.; Maruno, K.; Yeh, Y.-S.; Kuwata, H.; Tomita, K.; Goto, T.; Takahashi, N.; Kawada, T. Macrophage infiltration into obese adipose tissues suppresses the induction of UCP1 level in mice. *American Journal of Physiology-Endocrinology and Metabolism* **2016**, *310*, E676–E687, doi:10.1152/ajpendo.00028.2015.

84. Shan, B.; Wang, X.; Wu, Y.; Xu, C.; Xia, Z.; Dai, J.; Shao, M.; Zhao, F.; He, S.; Yang, L.; Zhang, M.; Nan, F.; Li, J.; Liu, J.; Liu, J.; Jia, W.; Qiu, Y.; Song, B.; Han, J. D. J.; Rui, L.; Duan, S. Z.; Liu, Y. The metabolic ER stress sensor IRE1α suppresses alternative activation of macrophages and impairs energy expenditure in obesity. *Nature Immunology* **2017**, *18*, 519–529, doi:10.1038/ni.3709.

85. da-Silva, W. S.; Ribich, S.; Drigo, R. A. e; Castillo, M.; Patti, M.-E.; Bianco, A. C. The chemical chaperones tauroursodeoxycholic and 4-phenylbutyric acid accelerate thyroid hormone activation and energy expenditure. *FEBS Letters* **2011**, *585*, 539–544, doi:10.1016/j.febslet.2010.12.044.

86. Contreras, C.; González-García, I.; Seoane-Collazo, P.; Martínez-Sánchez, N.; Liñares-Pose, L.; Rial-Pensado, E.; Fernø, J.; Tena-Sempere, M.; Casals, N.; Diéguez, C.; Nogueiras, R.; López, M. Reduction of hypothalamic endoplasmic reticulum stress activates browning of white fat and ameliorates obesity. *Diabetes* **2017**, *66*, 87–99, doi:10.2337/db15-1547.

87. Özcan, U.; Yilmaz, E.; Özcan, L.; Furuhashi, M.; Vaillancourt, E.; Smith, R. O.; Görgün, C. Z.; Hotamisligil, G. S. Chemical Chaperones Reduce ER stress and restore glucoes homeostasis in a mouse model of type 2 diabetes. *Science* **2006**, *313*, 1137–1140,

doi:10.1126/science.1128294.

88. Ohno, H.; Shinoda, K.; Spiegelman, B. M.; Kajimura, S. PPARγ agonists induce a white-to-brown fat conversion through stabilization of PRDM16 protein. *Cell Metabolism* **2012**, *15*, 395–404, doi:10.1016/j.cmet.2012.01.019.

89. Yuliana, A.; Jheng, H.-F.; Kawarasaki, S.; Nomura, W.; Takahashi, H.; Ara, T.; Kawada, T.; Goto, T. β-adrenergic Receptor Stimulation Revealed a Novel Regulatory Pathway via Suppressing Histone Deacetylase 3 to Induce Uncoupling Protein 1 Expression in Mice Beige Adipocyte. *International Journal of Molecular Sciences* **2018**, *19*, 2436, doi:10.3390/ijms19082436.

90. Gehart, H.; Kumpf, S.; Ittner, A.; Ricci, R. MAPK signalling in cellular metabolism: Stress or wellness? *EMBO Reports* **2010**, *11*, 834–840, doi:10.1038/embor.2010.160.

91. Burgermeister, E.; Seger, R. MAPK kinases as nucleo-cytoplasmic shuttles for PPARγ. *Cell Cycle* **2007**, *6*, 1539–1548, doi:10.4161/cc.6.13.4453.

92. Sakamoto, T.; Takahashi, N.; Sawaragi, Y.; Naknukool, S.; Yu, R.; Goto, T.; Kawada, T. Inflammation induced by RAW macrophages suppresses UCP1 mRNA induction via ERK activation in 10T1/2 adipocytes. *AJP: Cell Physiology* **2013**, *304*, C729–C738, doi:10.1152/ajpcell.00312.2012.

93. Salomone, S. Pleiotropic effects of glitazones: A double edge sword? *Frontiers in Pharmacology* **2011**, *MAR*, 1–6, doi:10.3389/fphar.2011.00014.

94. Digby, J. E.; Montague, C. T.; Sewter, C. P.; Sanders, L.; Wilkison, W. O.; O'Rahilly, S.; Prins, J. B. Thiazolidinedione exposure increases the expression of uncoupling protein 1 in cultured human preadipocytes. *Diabetes* **1998**, *47*, 138–141, doi:10.2337/diab.47.1.138.

95. Asano, H.; Kanamor, Y.; Higurashi, S.; Nara, T.; Kato, K.; Matsui, T.; Funaba, M. Induction of Beige-Like Adipocytes in 3T3-L1 Cells. *Journal of Veterinary Medical*

Science **2014**, *76*, 57–64, doi:10.1292/jvms.13-0359.

96. Miller, C. N.; Yang, J. Y.; England, E.; Yin, A.; Baile, C. A.; Rayalam, S. Isoproterenol increases uncoupling, glycolysis, and markers of beiging in mature 3T3-L1 adipocytes. *PLoS ONE* **2015**, *10*, 1–14, doi:10.1371/journal.pone.0138344.

97. Zhuo, X. Z.; Wu, Y.; Ni, Y. J.; Liu, J. H.; Gong, M.; Wang, X. H.; Wei, F.; Wang, T. Z.; Yuan, Z.; Ma, A. Q.; Song, P. Isoproterenol instigates cardiomyocyte apoptosis and heart failure via AMPK inactivation-mediated endoplasmic reticulum stress. *Apoptosis* **2013**, *18*, 800–810, doi:10.1007/s10495-013-0843-5.

98. Soccio, R. E.; Chen, E. R.; Lazar, M. A. Thiazolidinediones and the promise of insulin sensitization in type 2 diabetes. *Cell Metabolism* **2014**, *20*, 573–591, doi:10.1016/j.cmet.2014.08.005.

99. Urano, F.; Wang, X.-Z.; Bertolotti, A.; Zhang, Y.; Chung, P.; Harding, H. P.; Ron, D. Coupling of Stress in the Endoplasmic Reticulum to Activation of JNK Protein Kinases by Transmembrane Protein Kinase IRE1. *Science (New York, N.Y.)* **2000**, *287*, 664–666, doi:10.1126/science.287.5453.664.

100. Hauser, S.; Adelmant, G.; Sarraf, P.; Wright, H. M.; Mueller, E.; Spiegelman, B. M. Degradation of the peroxisome proliferator-activated receptor γ is linked to ligand-dependent activation. *Journal of Biological Chemistry* **2000**, *275*, 18527–18533, doi:10.1074/jbc.M001297200.

101. Camp, H. S.; Tafuri, S. R.; Leff, T.; Biology, C.; Biology, M. c-Jun N-Terminal Kinase Phosphorylates Peroxisome Proliferator-Activated Receptor- gamma 1 and Negatively Regulates Its Transcriptional Activity. *Endocrinology* **1999**, *140*, 392–397.

102. Molton, S. A.; Todd, D. E.; Cook, S. J. Selective activation of the c-Jun N-terminal kinase (JNK) pathway fails to elicit Bax activation or apoptosis unless the phosphoinositide 3′-

kinase (PI3K) pathway is inhibited. *Oncogene* **2003**, *22*, 4690–4701, doi:10.1038/sj.onc.1206692.

103. Kim, B. J.; Ryu, S. W.; Song, B. J. JNK- and p38 kinase-mediated phosphorylation of Bax leads to its activation and mitochondrial translocation and to apoptosis of human hepatoma HepG2 cells. *Journal of Biological Chemistry* **2006**, *281*, 21256–21265, doi:10.1074/jbc.M510644200.

104. Zinszner, H.; Kuroda, M.; Wang, X.; Batchvarova, N.; Lightfoot, R. T.; Remotti, H.; Stevens, J. L.; Ron, D. CHOP is implicated in programmed cell death in response to impaired function of the endoplasmic reticulum. *Genes and Development* **1998**, *12*, 982–995.

105. Guilherme, A.; Tesz, G. J.; Guntur, K. V. P.; Czech, M. P. Tumor necrosis factor-α induces caspase-mediated cleavage of peroxisome proliferator-activated receptor γ in adipocytes. *Journal of Biological Chemistry* **2009**, *284*, 17082–17091, doi:10.1074/jbc.M809042200.

106. Zha, B. S.; Zhou, H. ER stress and lipid metabolism in adipocytes. *Biochemistry Research International* **2012**, *2012*, doi:10.1155/2012/312943.

107. Travers, K. J.; Patil, C. K.; Wodicka, L.; Lockhart, D. J.; Weissman, J. S.; Walter, P. Functional and Genomic Analyses Reveal an Essential Coordination between the Unfolded Protein Response and ER-Associated Degradation. *Cell* **2000**, *101*, 249–258, doi:10.1016/S0092-8674(00)80835-1.

List of publications

- **Yuliana A**, Jheng HF, Kawarasaki S, Nomura W, Takahashi H, Ara T, Kawada T, and Goto T. β-adrenergic Receptor Stimulation Revealed a Novel Regulatory Pathway via Suppressing Histone Deacetylase 3 to Induce Uncoupling Protein 1 Expression in Mice Beige Adipocyte. *Int. J. Mol. Sci.* (2018), *19*(8):2436, 1-15. doi:10.3390/ijms19082436
- **Yuliana A**, Daijo A, Jheng HF, Kwon J, Nomura W, Takahashi H, Ara T, Kawada T, and Goto T. Endoplasmic Reticulum Stress Impaired Uncoupling Protein 1 Expression via the Suppression of Peroxisome Proliferator-Activated Receptor γ Binding Activity in Mice Beige Adipocytes. *Int. J. Mol. Sci.* (2019), *20*(2):274, 1-15. doi: 10.3390/ijms20020274

Others

- Yang HE, Li Y, Nishimura A, Jheng HF, **Yuliana A**, Ohue RK, Nomura W, Takahashi N, Kim CS, Yu R, Kitamura N, Park SB, Kishino S, Ogawa J, Kawada T, and Goto T. Synthesized Enone Fatty Acids Resembling Metabolites from Gut Microbiota Suppress Macrophage-Mediated Inflammation in Adipocytes. *Mol. Nutr. Food Res.* (2017), *61*(10), 1-13. doi: 10.1002/mnfr.201700064